

- Amaral K, et al. T0070907, a selective ligand for peroxisome proliferator-activated receptor  $\gamma$ , functions as an antagonist of biochemical and cellular activities. *J Biol Chem.* 2002;277:19649–19657.
- 11 Moser AR, Pitot HC, Dove WF. A dominant mutation that predisposes to multiple intestinal neoplasia in the mouse. *Science.* 1990;247:322–324.
  - 12 Peifer M. Beta-catenin as oncogene: the smoking gun. *Science.* 1997;275:1752–1753.
  - 13 Behrens J, von Kries JP, Kuhl M, Bruhn L, Wedlich D, Grosschedl R, et al. Functional interaction of beta-catenin with the transcription factor LEF-1. *Nature.* 1996;382:638–642.
  - 14 Barth AI, Nathke IS, Nelson WJ. Cadherins, catenins and APC protein: interplay between cytoskeletal complexes and signaling pathways. *Curr Opin Cell Biol.* 1997;9:683–690.
  - 15 Yost C, Torres M, Miller JR, Huang E, Kimelman D, Moon RT. The axis-inducing activity, stability, and subcellular distribution of beta-catenin is regulated in *Xenopus* embryos by glycogen synthase kinase 3. *Genes Dev.* 1996;10:1443–1454.
  - 16 de La Coste A, Romagnolo B, Billuart P, Renard CA, Buendia MA, Soubrane O, et al. Somatic mutations of the beta-catenin gene are frequent in mouse and human hepatocellular carcinomas. *Proc Natl Acad Sci U S A.* 1998;95:8847–8851.
  - 17 Korinek V, Barker N, Morin PJ, van Wichen D, de Weger R, Kinzler KW, et al. Constitutive transcriptional activation by a beta-catenin-Tcf complex in APC<sup>-/-</sup> colon carcinoma. *Science.* 1997;275:1784–1787.
  - 18 Miyoshi Y, Iwao K, Nagasawa Y, Aihara T, Sasaki Y, Imaoka S, et al. Activation of the beta-catenin gene in primary hepatocellular carcinomas by somatic alterations involving exon 3. *Cancer Res.* 1998;58:2524–2527.
  - 19 Nhieu JT, Renard CA, Wei Y, Cherqui D, Zafrani ES, Buendia MA. Nuclear accumulation of mutated beta-catenin in hepatocellular carcinoma is associated with increased cell proliferation. *Am J Pathol.* 1999;155:703–710.
  - 20 Kinzler KW, Vogelstein B. Lessons from hereditary colorectal cancer. *Cell.* 1996;87:159–170.
  - 21 Cadigan KM, Nusse R. Wnt signaling: a common theme in animal development. *Genes Dev.* 1997;11:3286–3305.
  - 22 Bennett CN, Ross SE, Longo KA, Bajnok L, Hemati N, Johnson KW, et al. Regulation of Wnt signaling during adipogenesis. *J Biol Chem.* 2002;277:30998–31004.
  - 23 Moldes M, Zuo Y, Morrison RF, Silva D, Park BH, Liu J, et al. Peroxisome-proliferator-activated receptor gamma suppresses Wnt/beta-catenin signalling during adipogenesis. *Biochem J.* 2003;376:607–613.
  - 24 Liu J, Wang H, Zuo Y, Farmer SR. Functional interaction between peroxisome proliferator-activated receptor gamma and beta-catenin. *Mol Cell Biol.* 2006;26:5827–5837.
  - 25 Jansson EA, Are A, Greicius G, Kuo IC, Kelly D, Arulampalam V, et al. The Wnt/beta-catenin signaling pathway targets PPARgamma activity in colon cancer cells. *Proc Natl Acad Sci U S A.* 2005;102:1460–1465.
  - 26 Shitashige M, Naishiro Y, Idogawa M, Honda K, Ono M, Hirohashi S, et al. Involvement of splicing factor-1 in beta-catenin/T-cell factor-4-mediated gene transactivation and pre-mRNA splicing. *Gastroenterology.* 2007;132:1039–1054.
  - 27 Sherr CJ. Mammalian G1 cyclins. *Cell.* 1993;73:1059–1065.
  - 28 Amati B, Alevizopoulos K, Vlach J. Myc and the cell cycle. *Front Biosci.* 1998;3:d250–d268.

# Inhibition of peroxisome proliferator-activated receptor $\gamma$ activity suppresses pancreatic cancer cell motility

Atsushi Nakajima,<sup>1,6</sup> Ayako Tomimoto,<sup>1</sup> Koji Fujita,<sup>1</sup> Michiko Sugiyama,<sup>1</sup> Hirokazu Takahashi,<sup>1</sup> Ikuko Ikeda,<sup>1</sup> Kunihiro Hosono,<sup>1</sup> Hiroki Endo,<sup>1</sup> Kyoko Yoneda,<sup>1</sup> Hiroshi Iida,<sup>1</sup> Masahiko Inamori,<sup>1</sup> Kensuke Kubota,<sup>1</sup> Satoru Saito,<sup>1</sup> Noriko Nakajima,<sup>2</sup> Koichiro Wada,<sup>3</sup> Yoji Nagashima<sup>4</sup> and Hitoshi Nakagama<sup>5</sup>

<sup>1</sup>Division of Gastroenterology, Yokohama City University School of Medicine, 3-9 Fuku-ura, Kanazawa-ku, Yokohama; <sup>2</sup>Department of Pathology, National Institute of Infectious Diseases, 1-23-1 Toyama, Shinjuku-ku, Tokyo; <sup>3</sup>Department of Pharmacology, Graduate School of Dentistry, Osaka University, 1-8 Yamadaoka, Suita, Osaka; <sup>4</sup>Department of Molecular Pathology, Yokohama City University Graduate School of Medicine, 3-9 Fuku-ura, Kanazawa-ku, Yokohama; <sup>5</sup>Biochemistry Division, National Cancer Center Research Institute, 1-1 Tsukiji 5-chome, Chuo-ku, Tokyo, Japan

(Received March 30, 2008/Revised June 6, 2008/Accepted June 9, 2008/Online publication October 9, 2008)

Peroxisome proliferator-activated receptor  $\gamma$  (PPAR $\gamma$ ) is a ligand-activated transcription factor that has been implicated in the carcinogenesis and progression of various solid tumors, including pancreatic carcinomas. We aimed to clarify the role of this receptor in pancreatic cell motility *in vitro* and in metastasis *in vivo*. Cell motility was examined by assaying transwell migration and wound filling in Capan-1 and Panc-1 pancreatic cancer cells, with or without the PPAR $\gamma$ -specific inhibitor T0070907. A severe combined immunodeficiency xenograft metastasis model was used to examine the *in vivo* effect of PPAR $\gamma$  inhibition on pancreatic cancer metastasis. In both transwell-migration and wound-filling assays, inhibition of PPAR $\gamma$  activity suppressed pancreatic cell motility without affecting *in vitro* cell proliferation. Inhibition of PPAR $\gamma$  also suppressed liver metastasis *in vivo* in metastatic mice. In PPAR $\gamma$ -inhibited cells, p120 catenin accumulation was induced predominantly in cell membranes, and the Ras-homologous GTPases Rac1 and Cdc42 were inactive. Inhibition of PPAR $\gamma$  in pancreatic cancer cells decreased cell motility by altering p120ctn localization and by suppressing the activity of the Ras-homologous GTPases Rac1 and Cdc42. Based on these findings, PPAR $\gamma$  could function as a novel target for the therapeutic control of cancer cell invasion or metastasis. (*Cancer Sci* 2008; 99: 1892–1900)

Pancreatic ductal adenocarcinoma is associated with one of the highest mortality rates in patients with malignancies.<sup>(1)</sup> Because of a lack of early symptoms, PDAC is often diagnosed only after a local tumor has disseminated and metastatic disease has already developed in regional lymph nodes or distant organ sites. To overcome this dismal situation, development of novel PDAC therapies involving drugs that target disease-specific molecules is urgently required. PPAR $\gamma$ , a member of the nuclear receptor family of ligand-activated transcription factors, is one promising target for such therapies.<sup>(2)</sup>

Activation of PPAR $\gamma$ , which is expressed mainly in adipose tissue, is known to play a central role in adipocyte differentiation and insulin sensitivity.<sup>(3)</sup> For this reason, synthetic PPAR $\gamma$ -activating ligands such as TZD are used commonly as oral antihyperglycemic agents to control non-insulin-dependent diabetes mellitus. More recently, PPAR $\gamma$  has been investigated as a target for the treatment of a variety of cancers.<sup>(4–6)</sup> The fact that PPAR $\gamma$  is overexpressed in many tumors, including examples in the esophagus, stomach, breast, lung, and colon, suggests that PPAR $\gamma$  function impacts tumor survival.<sup>(4–8)</sup> Initial efforts to alter PPAR $\gamma$  activity focused on activation with TZD ligands, which have been shown to induce G<sub>1</sub> cell-cycle arrest in a variety of tumor cell lines.<sup>(9,10)</sup> However, the reported benefits of

TZD for pancreatic carcinoma patients in clinical trials are modest at best.<sup>(11,12)</sup>

Several observations suggest that inhibition of PPAR $\gamma$  function may be beneficial in treating neoplasms.<sup>(13,14)</sup> Although PPAR $\gamma$  is overexpressed in many cancer cell types, loss-of-function mutations are rare,<sup>(15)</sup> which suggests that the receptor is a tumor cell survival factor. Evidence that PPAR $\gamma$  function can contribute to carcinogenesis or cancer cell survival includes reports of a murine colon cancer model in which PPAR $\gamma$  activation leads to increased tumor formation.<sup>(16,17)</sup>

Profiles of PPAR $\gamma$  expression in a variety of human malignancies, including pancreatic cancer, have been described. One recent report showed a significant association between high levels of PPAR $\gamma$  expression in pancreatic cancer cells and shorter overall survival time.<sup>(18)</sup> Prior investigations demonstrating that PPAR $\gamma$  inhibition induces apoptosis in epithelial tumor lines suggest strongly that PPAR $\gamma$  inhibition may also be beneficial in PDAC treatment.<sup>(19–21)</sup> In hepatocellular carcinoma cell lines, PPAR $\gamma$  inhibitors have been shown to inhibit cell adhesion and induce morphological changes that normally occur prior to the commitment to apoptosis; in contrast, caspase inhibitors do not prevent these changes.<sup>(20)</sup> We hypothesize that PPAR $\gamma$  inhibition interferes with adhesion-dependent epithelial cell survival signals, leading to cell death (anoikis). Two additional reports have shown that high doses of PPAR $\gamma$  inhibitors also interfere with Caco-2 cell survival.<sup>(22,23)</sup> The effect of PPAR $\gamma$  inhibitors (especially at low concentrations) on pancreatic cancer cells has not been investigated.

Ras-homologous GTPases play a pivotal role in the regulation of numerous cellular functions associated with malignant transformation and metastasis. Members of the Rho family of small GTPases are key regulators of actin reorganization and cell motility, as well as cell–cell and cell–extracellular matrix adhesion. These processes all play critical roles during the development and progression of cancer. Because of their pleiotropic functions, Rho proteins appear to be promising targets for the development of novel anticancer drugs,<sup>(24,25)</sup> including those for PDAC.<sup>(25)</sup> The ability to modulate pathways regulated by Rho could not only improve the therapeutic efficiency, but also reduce the side effects of conventional antineoplastic therapies.

<sup>6</sup>To whom correspondence should be addressed. E-mail: nakajima-ky@umin.ac.jp  
Abbreviations: FITC, fluorescein isothiocyanate; GST, glutathione-S-transferase; MTT, 3-[4,5-dimethylthiazol-2-yl]-2,5-diphenyltetrazolium bromide; p120ctn, p120 catenin; PDAC, pancreatic ductal adenocarcinoma cells; PPAR $\gamma$ , peroxisome proliferator-activated receptor  $\gamma$ ; PPRE, PPAR $\gamma$ -response element; Rho, Ras-homologous; SCID, severe combined immunodeficiency; siRNA, small interfering RNA; TZD, thiazolidinedione.

The protein p120ctn is the prototypic member of a subfamily of armadillo repeat-domain proteins involved in intercellular adhesion. A recent report demonstrated clearly that p120 regulates, at least in part, the activity of Rho GTPases, and that p120 association with classical cadherins regulates their stability.<sup>(26)</sup> Ectopic expression of p120ctn has been shown to promote cell migration and to induce a wide variety of morphological changes.<sup>(26)</sup>

In the present study, we investigated the effects of PPAR $\gamma$  inhibitors on pancreatic cell lines and xenograft metastatic tissues that function as models for PDAC. Our data demonstrate that inhibition of PPAR $\gamma$  in pancreatic cancer cells decreases cell motility by altering p120ctn localization and suppressing the activity of the Rho GTPases Rac1 and Cdc42. These findings suggest that PPAR $\gamma$  inhibitors may improve the benefit of current PDAC therapeutics.

## Materials and Methods

**Cell lines and reagents.** The PDAC cell line Panc-1 was purchased from the American Type Culture Collection (Rockville, MD, USA). Other cell lines were provided by the Cell Resource Center for Biomedical Research, Tohoku University (Sendai, Japan). All cell lines were grown in RPMI-1640 (Sigma-Aldrich, St Louis, MO, USA) supplemented with 10% fetal bovine serum. Cells were maintained at 37°C in an atmosphere of humidified air with 5% CO<sub>2</sub>. The PPAR $\gamma$ -specific inhibitor T0070907 and PPAR $\gamma$  ligand rosiglitazone were purchased from Cayman Chemical (Ann Arbor, MI, USA).

**Western blot analysis.** Adherent cells were washed in phosphate-buffered saline, and cell extracts were prepared in Laemmli lysis buffer. Protein concentrations were measured using Bio-Rad Protein Assay Reagent (Bio-Rad, Richmond, CA, USA) following the manufacturer's suggested procedure. After electrophoresis of extract aliquots (20  $\mu$ g protein) on 10% sodium dodecylsulfate-polyacrylamide gels, proteins were transferred to nitrocellulose membranes (Millipore, Bedford, MA, USA), blocked at room temperature for 1 h in Tris-buffered saline with 5% bovine serum albumin, and then incubated with primary monoclonal antibody for 1 h. Anti-PPAR $\gamma$  antibody (E-8) was purchased from Santa Cruz Biotechnology (Santa Cruz, CA, USA); monoclonal antibodies against p120ctn and Rac1 were obtained from BD Transduction Laboratories (Palo Alto, CA, USA). After three washes the membranes were incubated for 1 h at room temperature with secondary antibody, and immune complexes were visualized using the enhanced chemiluminescence detection kit (Amersham, London, UK) following the manufacturer's procedure. Images were captured and analyzed using a LAS-3000 imaging system (Fujifilm, Tokyo, Japan). The ProteoExtract Subcellular Proteome Extraction Kit (EMD Biosciences, Darmstadt, Germany) was used for the preparation of cytosolic protein extracts.

**Cell proliferation and apoptosis assays.** Cell proliferation was measured using MTT assays.<sup>(27)</sup> Approximately  $5 \times 10^3$  cells in 100  $\mu$ L medium were plated per well in a 96-well plate. After 24 h incubation, the medium was changed and supplemented with various concentrations of T0070907 in dimethylsulfoxide, and the cells were incubated for another 24–72 h. After incubating the plates for an additional 4 h with MTT solution (0.5%), sodium dodecylsulfate was added to a final concentration of 20% and absorbance at 595 nm was determined for each well using a microplate reader (Model 550; Bio-Rad). Control wells were treated with dimethylsulfoxide alone. Three independent experiments were carried out for each cell line. Annexin V staining with the annexin V-FITC apoptosis detection kit (Becton Dickinson, San Jose, CA, USA) followed by FACScan flow cytometry (Becton Dickinson) was used to identify apoptotic cells. Apoptosis measures were carried out in triplicate.

**Cell-motility assays.** Motility was assessed by migration of cells in porous-membrane culture inserts (8.0- $\mu$ m pore size; Becton Dickinson). After 24 h of incubation, cells that did not migrate were removed from the upper surface of the membrane with a cotton swab, and migrating cells on the lower surface of the membrane were fixed and stained with toluidine blue. Migrating cell counts were estimated from counts of three independent microscopic visual fields ( $\times 100$ ). To estimate cell-migration activity during wound healing, cells were grown for 2 days (to confluency), after which a scrape in the form of a cross was made through the confluent monolayers with a plastic pipette tip. To measure migration, several wounded areas within each plate were marked for orientation and then photographed periodically by phase-contact microscopy for 24 h after wounding.

**Inhibition of PPAR $\gamma$  function using siRNA.** PPAR $\gamma$  siRNA was purchased from Santa Cruz Biotechnology. Panc-1 and Capan-1 cells at 70% confluence were transfected with PPAR $\gamma$  siRNA using Lipofectamine 2000 (Invitrogen, Carlsbad, CA, USA) in accordance with the manufacturer's protocol. The cells were treated with 10 nmol/L PPAR $\gamma$  siRNA for 24 h. Stealth RNAi Negative Control Medium GC (Invitrogen) was used for control specimens. Using real-time reverse transcription-polymerase chain reaction to measure steady-state mRNA levels in cells, PPAR $\gamma$ -specific siRNA was found to inhibit PPAR $\gamma$  expression to levels less than 30% of those in control cells (data not shown).

**Measuring the effect of T0070907 on PPAR $\gamma$ -dependent transcription.** Capan-1 cells transfected with plasmid encoding a PPAR $\gamma$ -response element fused to a luciferase reporter (pHD[ $\times 3$ ]PPRE-Luc) were stimulated as described previously with 1  $\mu$ mol/L rosiglitazone and various concentrations of T0070907.<sup>(20)</sup> Luciferase activity was measured 16 h after transfection. Because Renilla luciferase control plasmids are sensitive to steroid/thyroid/retinoid nuclear-receptor stimulation, variability in transfection efficiencies (<20%) were assessed in parallel experiments using the pRL-TK plasmid (Promega, Madison, WI, USA).

**Immunofluorescence staining.** Cells ( $5 \times 10^5$  per well) were grown on collagen-1-coated glass coverslips in six-well flat-bottom plates for 24 h. After 24 h incubation, T0070907 was added to a final concentration of 0.1  $\mu$ mol/L and the cells were grown for an additional 24 h. The cells were then fixed in 4% paraformaldehyde followed by 100% ethanol at -20°C. After permeabilization with 0.1% Triton-X, non-specific binding of antibody to the cells was blocked with 2% normal swine serum. Cells were incubated subsequently with anti-p120 catenin antibody followed by FITC-labeled secondary antibody. Samples were then mounted using Vectashield (Vector Laboratories, Burlingame, CA, USA) and examined using confocal laser-scanning microscopy (Carl Zeiss, Oberkochen, Germany). All experiments were repeated in triplicate.

**Measurement of Rac-1 and Cdc42 activities.** GST pull-down assays using a Rac-1/Cdc42 activation kit were used to evaluate Rac1/Cdc42 activities according to the manufacturer's protocol (Stressgen, Ann Arbor, MI, USA). Briefly, we used a GST fusion polypeptide composed of GST fused to the interactive domain of human p21-activated kinase-1, which interacts specifically with GTP-bound Cdc42 and Rac1 GTPases.<sup>(25)</sup> The GST fusion target was incubated with cell lysates and then applied to GST-specific beads to estimate the relative abundance of active Cdc42 and Rac1. Bound Rac1 and Cdc42 proteins were resolved on 12% denaturing polyacrylamide gels and distinguished by western blotting using antibodies specific to each protein. The amount of active GTP-bound enzyme was quantified relative to the total amount of each GTPase present in whole unprecipitated cell lysates. The experiments were carried out six times.

**In vivo metastasis study.** Five-week-old male SCID mice were obtained from CLEA Japan (Tokyo, Japan) and maintained in a

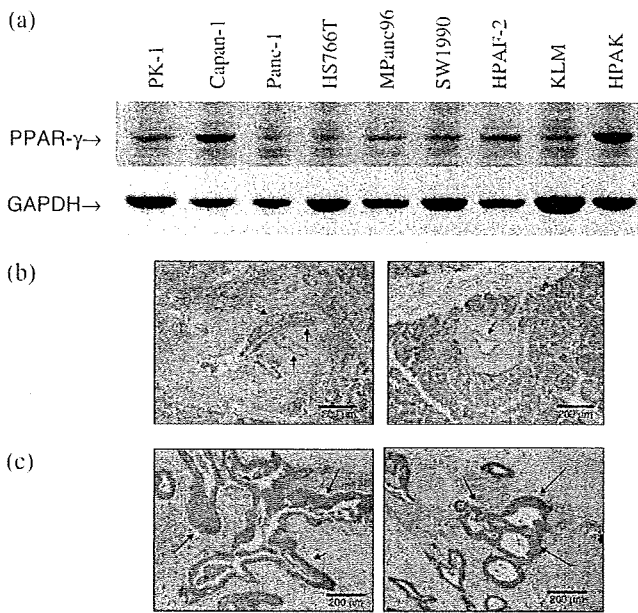


**Fig. 1.** Expression of peroxisome proliferator-activated receptor  $\gamma$  (PPAR $\gamma$ ) in pancreatic cancer cells. (a) Western blots showing PPAR $\gamma$  expression in various pancreatic ductal adenocarcinoma cell lines, as well as a glyceraldehyde-3-phosphate dehydrogenase (GAPDH) internal control. Immunohistochemical staining of (b) normal ductal epithelium (left and right panels) and (c) pancreatic ductal adenocarcinoma (left and right panels) with anti-PPAR $\gamma$  antibody. Arrows mark staining of normal pancreatic ductal epithelium in (b) and pancreatic ductal adenocarcinoma in (c).

specific pathogen-free environment. Experiments were carried out according to the guidelines of Yokohama City University. Six-week-old mice were used in this experiment. To assay metastatic capability, viable cancer cells were suspended in serum-free medium, and 20- $\mu$ L aliquots of cell suspension containing  $2 \times 10^6$  cells were inoculated into the spleens of SCID mice under anesthesia. After inoculation, the mice were randomized into two treatment groups ( $n = 6$ ) and one control group ( $n = 6$ ). Administration of T0070907 (5 mg/kg/day) to each treatment group began 1 day after cell inoculation and continued daily for 4 weeks. Four weeks after inoculation, the mice were killed and autopsied immediately. Liver metastasis was measured by counting macroscopic lesions, and measuring them to calculate tumor volume:

$$\text{length}/2 \times \text{width}/2 \times \text{height}/2 \times 4/3 \times \pi.^{(28)}$$

Examination of hematoxylin–eosin-stained sections of each lesion resulted in assessments of histopathological alterations in liver metastases.

## Results

### Expression of PPAR $\gamma$ in pancreatic ductal adenocarcinoma cells.

Western blotting of PPAR $\gamma$  with the E8 antibody revealed a specific band between 50 and 60 kDa present in all PDAC cell lines examined (Fig. 1a). Among these lines, steady-state levels of PPAR $\gamma$  protein were highest in Capan-1 and HPAK cells, and lowest in Panc-1 and HS766T cells. Immunohistochemical staining with a PPAR $\gamma$ -specific antibody demonstrated that PPAR $\gamma$  expression in PDAC tissues (Fig. 1c) was similar to normal pancreatic ductal epithelium (Fig. 1b).

**Peroxisome proliferator-activated receptor  $\gamma$  inhibitors reduce migration of PDAC cells.** The effect of the PPAR $\gamma$  antagonist

T0070907 on PDAC cell migration was measured using *in vitro* wound-filling assays. The migration of wounded cells treated with T0070907 was inhibited significantly (Fig. 2a,b) relative to untreated, wounded Capan-1 and Panc-1 cells. Among cells transfected with PPAR $\gamma$  siRNA to reduce PPAR $\gamma$  expression levels, Capan-1 cell migration was more severely inhibited than Panc-1 (Fig. 2c,d). These results indicate that chemical inhibitors or inhibitory siRNA molecules that reduce PPAR $\gamma$  activity lead to inhibition of wound filling. Migration of Capan-1 and Panc-1 cells in the absence or presence of several concentrations of T0070907 were also measured in 24-h transwell migration assays (Fig. 3). In both cell lines, the presence of T0070907 reduced cell migration significantly and in a dose-dependent manner (Fig. 3a,c). Reduced migration of cells with PPAR $\gamma$  siRNA relative to untreated controls (Fig. 3b,d) demonstrates that transwell migration is inhibited specifically by a reduction in PPAR $\gamma$  activity.

**Effect of PPAR $\gamma$  inhibitor on cell proliferation and apoptosis.** To investigate whether chemical inhibition of PPAR $\gamma$  affects cancer cell proliferation and apoptosis, we used MTT assays to measure cell proliferation and apoptosis in cultured Panc-1 and Capan-1 PDAC cell lines. No significant changes in cell proliferation (Fig. 4a,b) or apoptosis (Fig. 4c,d) were observed in T0070907-treated versus untreated PDAC cells. These results demonstrate that suppression of cell proliferation or apoptosis is not necessarily consequent to T0070907-mediated suppression of PDAC cell motility.

**Inhibition of PPAR $\gamma$  alters the subcellular localization of p120ctn.** Association of p120ctn with the intracellular domains of cadherins promotes cell–cell adhesion and cell motility by regulating the activation of Rho GTPases.<sup>(29,30)</sup> Because cytoplasmic p120ctn is the only known activator of Rho GTPases that functions in cell motility, the ratio of cadherin-bound p120ctn to p120ctn in the cytoplasmic pool is an important factor regulating motility. To examine the involvement of p120ctn in T0070907-mediated suppression of cell motility, we used immunocytochemical analyses to examine the subcellular distribution of p120ctn in PDAC cells. In T0070907-treated Capan-1 cells, p120ctn was found predominantly on the plasma membranes (relative to more free p120ctn in the cytoplasm of untreated cells) (Fig. 5a). In contrast, there were no significant changes in the distribution of p120ctn in T0070907-treated Panc-1 cells (data not shown). The intracellular distributions of PPAR $\gamma$  and p120ctn did not overlap (merged) (Fig. 5a).

Although western blots of fractionated cells revealed that cytoplasmic p120ctn levels decreased in T0070907-treated Capan-1 cells (Fig. 5b), no significant change in distribution was observed between untreated and treated Panc-1 cells (data not shown). These results indicate that in Capan-1 cells, PPAR $\gamma$  inhibition increases the relative amount of cadherin-bound p120ctn. We speculate that relatively low levels of PPAR $\gamma$  expression in Panc-1 cells may confound our ability to measure any similar change in p120ctn subcellular localization following T0070907 treatment. To investigate whether PPAR $\gamma$  activity in Capan-1 cells is inhibited by low concentrations of T0070907, the effect of a range of T0070907 concentrations on PPRE-dependent transcription was measured (Fig. 5c). With 0.1  $\mu$ mol/L T0070907, PPRE-dependent transcription in Capan-1 cells was inhibited to approximately half maximum.

**Peroxisome proliferator-activated receptor  $\gamma$  inhibitor suppresses the activity of Rac-1 and Cdc42.** Previous reports suggest that p120ctn affects cell motility in association with Rac1 and Cdc42 Rho GTPases.<sup>(30–33)</sup> The activities of Rac1 and Cdc42 GTPases were measured in lysates of T0070907-treated and -untreated Capan-1 cells using a GST pull-down target that interacts specifically with active GTPases. In T0070907-treated cells, we observed a significant decrease in the percent-active fractions of Rac1 and Cdc42 GTPases (Fig. 6).

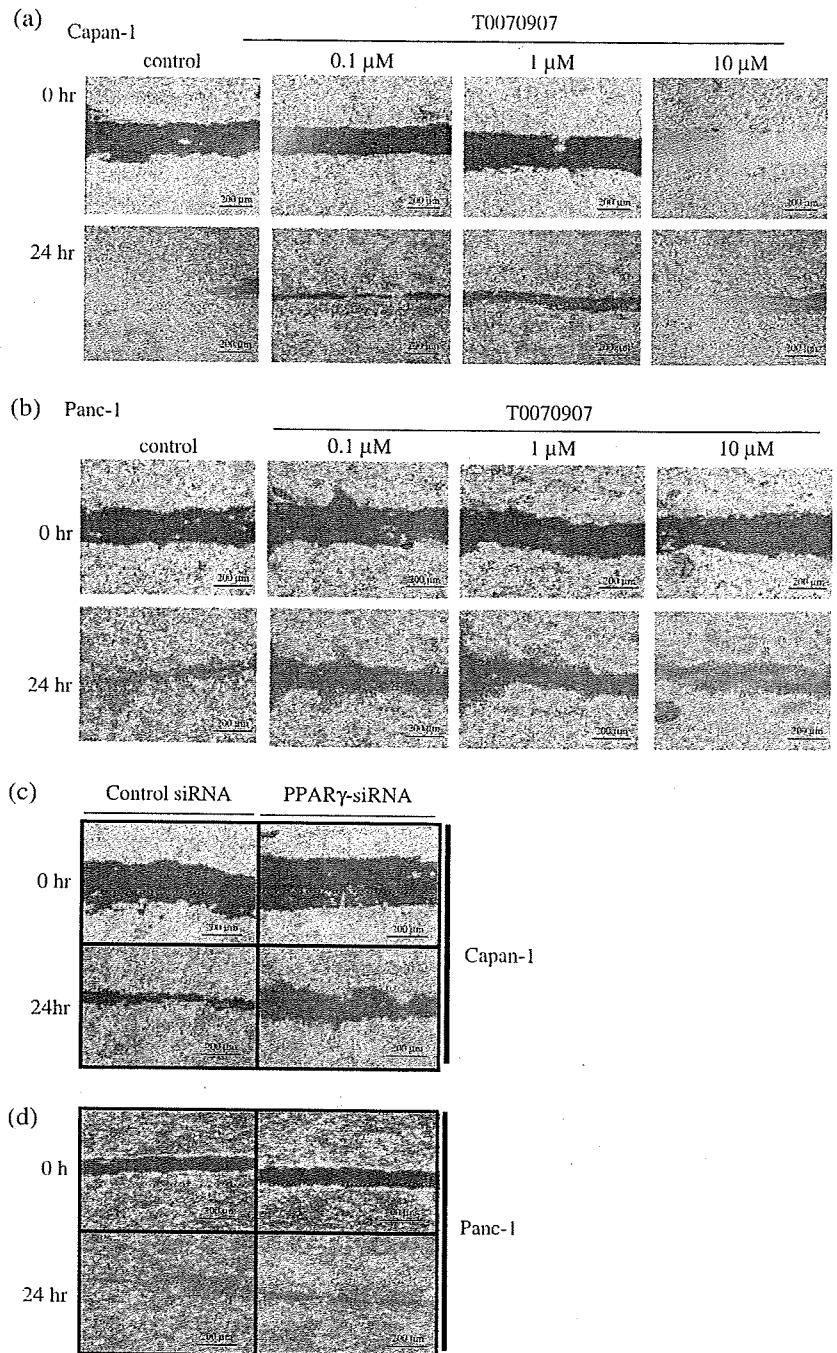


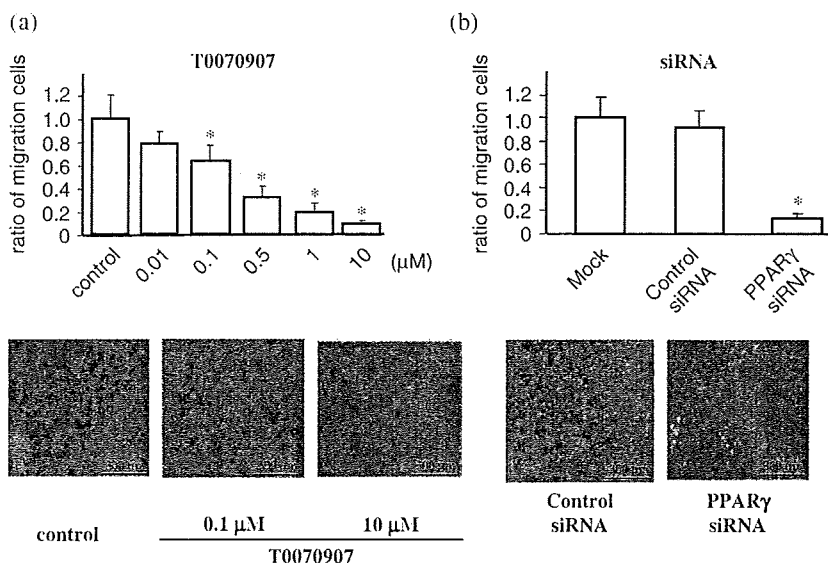
**Fig. 2.** Peroxisome proliferator-activated receptor  $\gamma$  (PPAR $\gamma$ ) inhibition reduces the wound-filling ability of PDAC cells. Wound-filling assays in (a) Capan-1 and (b) Panc-1 cells treated with various concentrations of T0070907 for 24 h. In both lines, all concentrations of PPAR $\gamma$  inhibitor result in slower cell migration into wound areas. (c) Capan-1 and (d) Panc-1 cells transfected with PPAR $\gamma$  small interfering RNA (siRNA) also migrated more slowly into wound areas than cells transfected with control siRNA.

**Peroxisome proliferator-activated receptor  $\gamma$  inhibitor reduces liver metastasis in a mouse xenograft model.** To investigate whether PPAR $\gamma$  inhibitors affect metastatic cell spreading, we tested the ability of T0070907 to reduce metastatic tumor formation in a Capan-1/SCID mouse xenograft model. Capan-1 cells were injected into the spleens of SCID mice, and the number and size of metastatic lesions in livers were measured after 4 weeks (Fig. 7). Mice treated orally with 5 mg/kg/day of T0070907 contained two-thirds fewer metastatic foci ( $P < 0.05$ ), with an average tumor volume of only 12% of tumors in control mice ( $P < 0.05$ ) (Table 1). Serum L-alanine aminotransferase (ALT) levels were within the normal range in the all mice (Suppl. Fig. S1).

## Discussion

We demonstrated that levels of PPAR $\gamma$  expression vary among pancreatic adenocarcinoma cell lines (Fig. 1) and tested the effect of the PPAR $\gamma$ -specific inhibitor T0070907 on PDAC cells. In Capan-1 and Panc-1 cells, both T0070907 and PPAR $\gamma$  siRNA suppressed cell motility, migration, and invasion, but did not inhibit cell proliferation (Figs 2–4). These results suggest strongly that PPAR $\gamma$  plays a crucial role in PDAC cell motility, migration, and invasion. Elucidating the mechanism that underlies cell motility is of clinical importance as a means for controlling tumor cell invasion, dissemination, and metastasis in patients with pancreatic cancer.

## Capan-1



## Panc-1

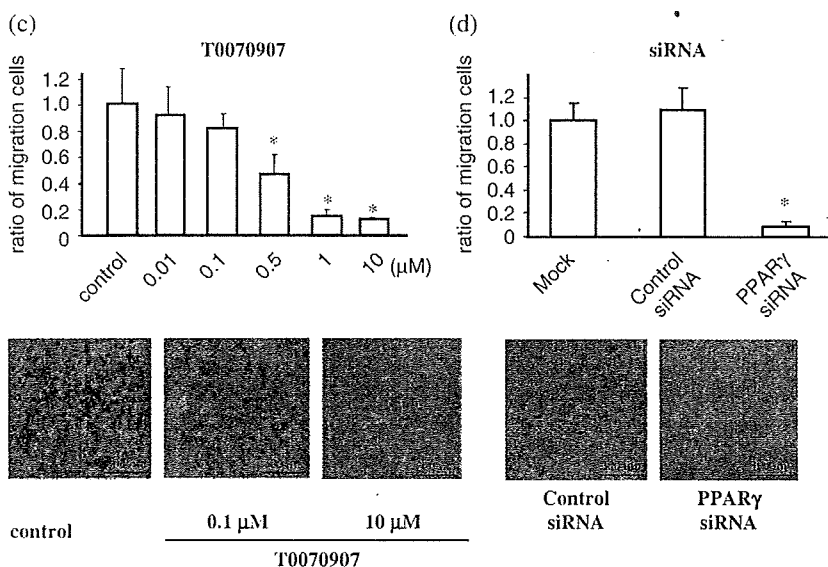


**Fig. 3.** Peroxisome proliferator-activated receptor  $\gamma$  (PPAR $\gamma$ ) inhibition reduces migration of PDAC cells. Cell migrations were estimated from transwell migration assays, in which migrated cells are stained violet and membrane pores can be seen as white dots. Relative to control-treated cells, (a) Capan-1 and (c) Panc-1 cell migration decreased significantly and in a dose-dependent manner in response to increasing concentrations of PPAR $\gamma$  inhibitor T0070907 (\* $P < 0.05$ ). (b,d) Significant decreases in cell migration were also observed in PPAR $\gamma$  small interfering RNA (siRNA)-transfected cells relative to control siRNA-transfected cells.

**Table 1.** Effects of peroxisome proliferator-activated receptor  $\gamma$  inhibitor (T0070907) on liver metastasis of Capan-1 cells

Incidence	Number of metastatic colonies (mean $\pm$ SD)	Total tumor volume (mm <sup>3</sup> ) (mean $\pm$ SD)
Vehicle	3.50 $\pm$ 1.05	738.6 $\pm$ 415.7
T0070907 (5 mg/kg/day)	1.00 $\pm$ 1.27 $P < 0.05$	86.8 $\pm$ 173.2 $P < 0.05$

Capan-1 cells were injected into the spleen of male severe combined immunodeficiency mice. One day after injection, three groups ( $n = 6$ ) were randomized into vehicle or 5 mg/kg/day T0070907. After 4 weeks, livers were harvested, and the number of metastases and total tumor volume of all metastatic lesions was determined.

Following treatment with T0070907 PPAR $\gamma$  inhibitor, p120ctn was found predominantly in Capan-1 cell membranes. Recent reports demonstrate that p120ctn associates with all classic cadherin subtypes, and is involved in the regulation of cell motility and cell

adhesion.<sup>(26)</sup> p120ctn is known to also regulate actin cytoskeleton configuration. We did not observe colocalization of PPAR $\gamma$  and p120ctn expression in PPAR $\gamma$  inhibitor-treated or -untreated cells, indicating that PPAR $\gamma$  may not interact directly with p120ctn.

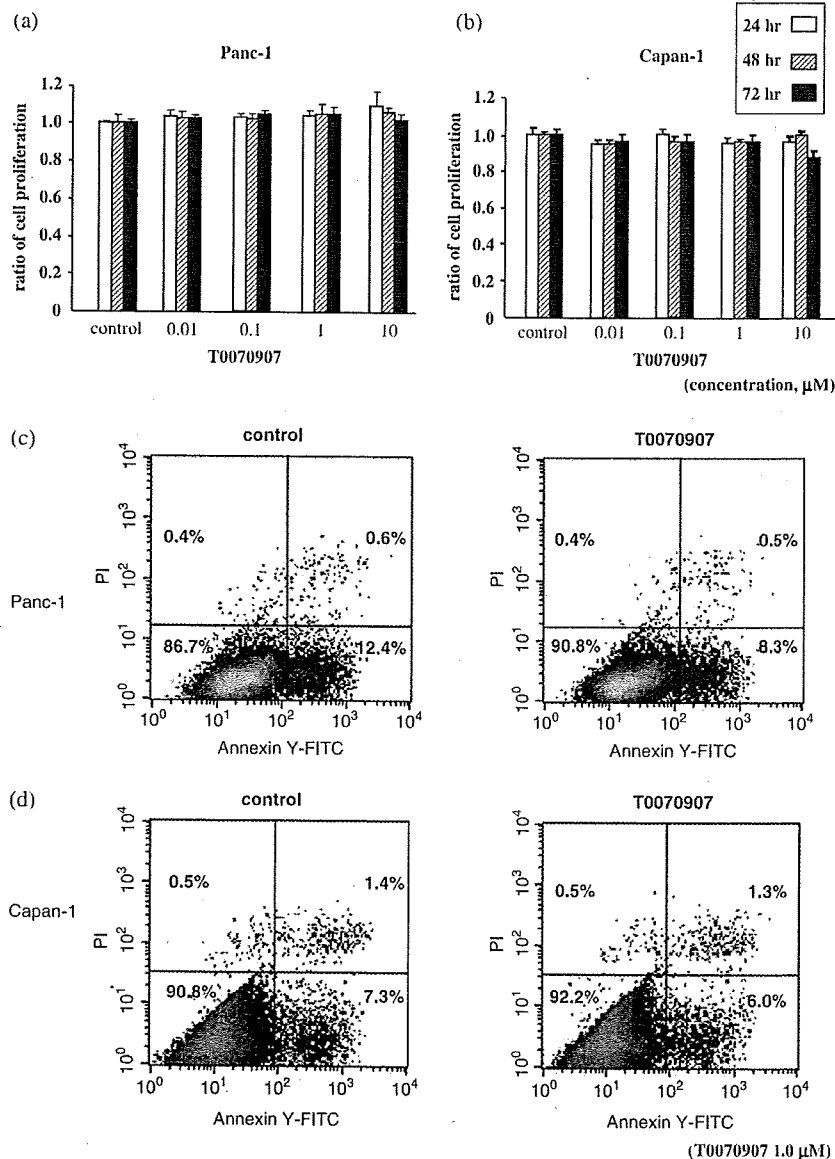


**Fig. 4.** Effect of a peroxisome proliferator-activated receptor  $\gamma$  (PPAR $\gamma$ ) inhibitor on cell proliferation and apoptosis in PDAC cells. Cell proliferation was calculated from 3-[4,5-dimethylthiazol-2-yl]-2,5-diphenyltetrazolium bromide (MTT) assays. (a) Panc-1 and (b) Capan-1 cells treated with 1.0  $\mu\text{mol/L}$  T0070907 for 24, 48, and 72 h showed no significant change in MTT values relative to control cells (y-axis values represent the ratio of MTT optical density readings from treated and untreated cells; columns represent ratio mean  $\pm$  SD). Apoptotic cell counts were measured by fluorescence activated cell sorting (FACS) after treatment of (c) Panc-1 or (d) Capan-1 cells without or with 1.0  $\mu\text{mol/L}$  T0070907 for 24 h. T0070907 treatments did not result in any significant changes in the percentage of apoptotic cells.

Ras-homologous GTPases, which localize to membranes in a GDP-bound state, are activated to a GTP-bound state upon stimulation of cell-surface receptors. Upon activation, Rho GTPases bind effectors that trigger specific cellular responses. As Rho proteins are known to play essential roles in signaling events that regulate cadherin-dependent motility, specific inhibitors of individual Rho functions (notably RhoA-, RhoB-, Rac1-, or Cdc42-related functions) could provide therapeutic benefits in controlling cancer metastasis. Indeed, compounds developed as specific inhibitors of the RhoA-effector molecule Rho-kinase have been demonstrated to exert antimetastatic activity *in vivo*.<sup>(24)</sup>

The inactivation of Rac1 and Cdc42 that we observed in response to PPAR $\gamma$  inhibition indicates that these molecules are involved in PPAR $\gamma$ -mediated PDAC cell motility. We also demonstrated liver metastasis inhibition in response to PPAR $\gamma$  inhibition in an *in vivo* metastatic model. Previous reports have demonstrated an induction in apoptosis in response to PPAR $\gamma$  inhibition in other epithelial tumor lines.<sup>(19-21)</sup> Anoikis, which is a loss of adhesion-induced apoptosis, was also reported in response to PPAR $\gamma$  inhibition by T0070907; however, concen-

trations greater than 10  $\mu\text{mol/L}$  T0070907 have been shown to be required to induce anoikis in a variety of carcinoma cell lines. In the present study, we observed a significant inhibitory effect of T0070907 on cell migration at much lower T0070907 concentrations (0.01–1  $\mu\text{mol/L}$ ; Fig. 5c) that had no effect on cell proliferation or cell death as measured in MTT and apoptosis assays (Fig. 4). Our findings at low concentrations of T0070907 suggest that inhibition of cancer cell migration is due to the specificity of T0070907's pharmacological effect on PPAR $\gamma$ , and not by anoikis, which is induced at higher concentrations of PPAR $\gamma$  inhibitor. The relatively low concentrations of T0070907 required for inhibition and the dose-dependent effect of the inhibitor on cell migration make it unlikely that inhibition was non-specific.

Transwell migration and wound-filling assays in both Capan-1 and Panc-1 pancreatic cancer cell lines demonstrated the inhibitory effects of PPAR $\gamma$  on cell motility *in vitro*. In contrast, the effects of PPAR $\gamma$  inhibitor on p120ctn subcellular localization, and on Rac1 and Cdc42 GTPase activities, were exclusive to Capan-1 cells, and not seen in Panc-1. We speculate that relative

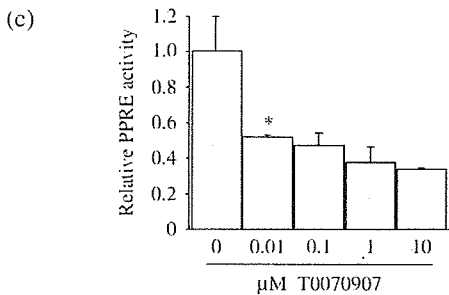
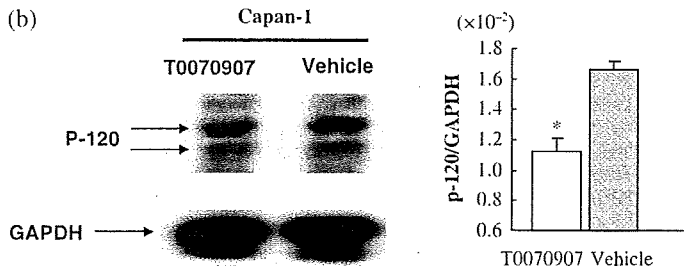
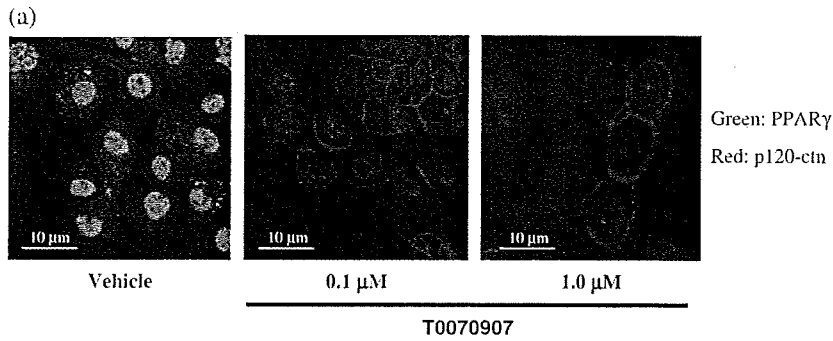


**Fig. 5.** Peroxisome proliferator-activated receptor  $\gamma$  (PPAR $\gamma$ ) inhibitor T0070907 affects the subcellular localization of p120 catenin (p120ctn) in Capan-1 cells. (a) The subcellular distribution of p120ctn in Capan-1 control cells or those treated with 0.1 or 1.0  $\mu$ mol/L T0070907 were compared following immunostaining with anti-p120ctn (red) and anti-PPAR $\gamma$  (green). Although p120ctn accumulated in the cytoplasm of vehicle-treated cells, it localized predominantly to cell membranes in T0070907-treated Capan-1 cells. Merged images of PPAR $\gamma$  and p120ctn immunohistochemical staining patterns show no colocalization. (b) Western-blot analysis of cytosolic protein extracts with p120ctn antibody and glyceraldehyde-3-phosphate dehydrogenase (GAPDH) control antibody. T0070907 treatment resulted in reduced signal strength from the cytosolic p120ctn band. Changes in the cytosolic p120ctn expression can be seen by the reduction in the ratio of p120ctn:GAPDH signal strength  $\pm$  SD. \* $P < 0.05$ . (c) Capan-1 cells transfected with a PPAR $\gamma$ -response element (PPRE)-luciferase reporter plasmid were stimulated with 1 mmol/L rosiglitazone (synthetic ligand of PPAR $\gamma$ ) in the presence of concentrations of T0070907 shown. Luciferase activity was measured after 16 h of treatment. Bars represent relative PPARE activity as measured by the ratio of PPAR $\gamma$ -dependent luciferase activity in treated cells relative to untreated cells.

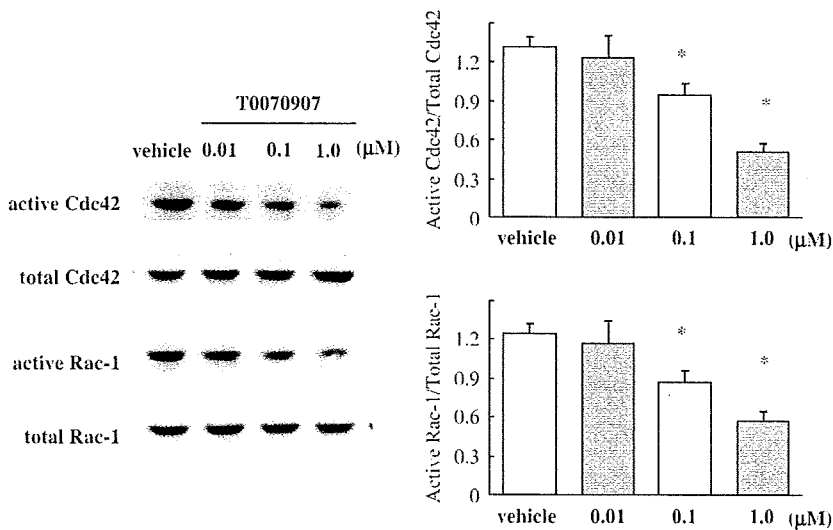
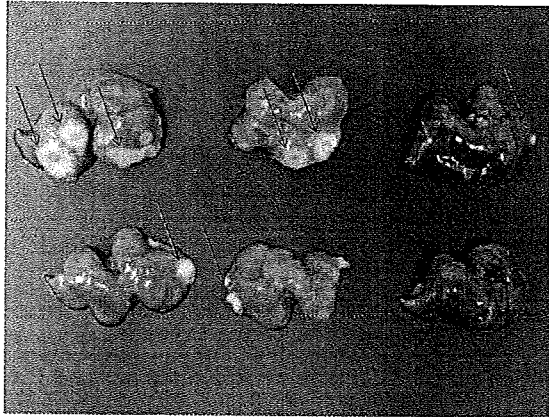


**Fig. 6.** Effect of the peroxisome proliferator-activated receptor  $\gamma$  (PPAR $\gamma$ ) inhibitor T0070907 on the activity of Rac-1 and Cdc42 GTPases in Capan-1 cells. GTPase activity for Rac-1 and Cdc42 was measured using GST pull-down assays that are capable of distinguishing the percentage of the active fraction (relative to total) of Rac-1 and Cdc42 in lysates of Capan-1 cells. Treatment with T0070907 (0.1 and 1.0  $\mu$ mol/L) resulted in a significant decrease in the percentage of active Rac-1 and Cdc42. Each column represents the mean  $\pm$  SD. The experiments were carried out six times. \* $P < 0.05$ .





Vehicle      T0070907 (1 mg/kg/day)      T0070907 (5 mg/kg/day)

**Fig. 7.** Peroxisome proliferator-activated receptor  $\gamma$  (PPAR $\gamma$ ) inhibitor T0070907 reduces the number and volume of metastases in a murine xenograft model. Numbers and areas of metastases (arrows) in the liver decreased markedly in mice treated with T0070907 relative to control mice.

## References

- Jemal A, Siegel R, Ward E, Murray T, Xu J, Thun MJ. Cancer statistics, 2007. *CA Cancer J Clin* 2007; **57**: 43–66.
- Kersten S, Desvergne B, Wahli W. Roles of PPARs in health and disease. *Nature* 2000; **405**: 421–4.
- Desvergne B, Wahli W. Peroxisome proliferator-activated receptors: nuclear control of metabolism. *Endocr Rev* 1999; **20**: 649–88.
- Takahashi T, Fujiwara Y, Higuchi K *et al.* PPAR- $\gamma$  ligands inhibit growth of human esophageal adenocarcinoma cells through induction of apoptosis, cell cycle arrest and reduction of ornithine decarboxylase activity. *Int J Oncol* 2001; **19**: 465–71.
- Chang TH, Szabo E. Induction of differentiation and apoptosis by ligands of peroxisome proliferator-activated receptor gamma in non-small cell lung cancer. *Cancer Res* 2000; **60**: 1129–38.
- DuBois RN, Gupta R, Brockman J, Reddy BS, Krakow SL, Lazar MA. The nuclear eicosanoid receptor, PPAR $\gamma$ , is aberrantly expressed in colonic cancers. *Carcinogenesis* 1998; **19**: 49–53.
- Mueller E, Sarraf P, Tontonoz P *et al.* Terminal differentiation of human breast cancer through PPAR gamma. *Mol Cell* 1998; **1**: 465–70.
- Sato H, Ishihara S, Kawashima K *et al.* Expression of peroxisome proliferator-activated receptor (PPAR)  $\gamma$  in gastric cancer and inhibitory effects of PPAR $\gamma$  agonists. *Br J Cancer* 2000; **83**: 1394–400.
- Guan YF, Zhang YH, Breyer RM, Davis L, Breyer MD. Expression of peroxisome proliferator-activated receptor  $\gamma$  (PPAR $\gamma$ ) in human transitional bladder cancer and its role in inducing cell death. *Neoplasia* 1999; **1**: 330–9.
- Kitamura S, Miyazaki Y, Shinomura Y, Kondo S, Kanayama S, Matsuzawa Y. Peroxisome proliferator-activated receptor  $\gamma$  induces growth arrest and differentiation markers of human colon cancer cells. *Jpn J Cancer Res* 1999; **90**: 75–80.
- Debrock G, Vanhentenrijk V, Sciort R, Debiec-Rychter M, Oyen R, Van Oosterom A. A phase II trial with rosiglitazone in liposarcoma patients. *Br J Cancer* 2003; **89**: 1409–12.
- Kulke MH, Demetri GD, Sharpless NE *et al.* A phase II study of troglitazone, an activator of the PPAR $\gamma$  receptor, in patients with chemotherapy-resistant metastatic colorectal cancer. *Cancer J* 2002; **8**: 395–9.
- Martelli ML, Iuliano R, Le Pera I *et al.* Inhibitory effects of peroxisome proliferator-activated receptor  $\gamma$  on thyroid carcinoma cell growth. *J Clin Endocrinol Metab* 2002; **87**: 4728–35.
- Panigrahy D, Shen LQ, Kieran MW, Kaipainen A. Therapeutic potential of thiazolidinediones as anticancer agents. *Expert Opin Invest Drugs* 2003; **12**: 1925–37.
- Posch MG, Zang C, Mueller W, Lass U, von Deimling A, Elstner E. Somatic mutations in peroxisome proliferator-activated receptor- $\gamma$  are rare events in human cancer cells. *Med Sci Monit* 2004; **10**: BR250–4.

to Panc-1 cells, steady-state levels of PPAR $\gamma$  in Capan-1 cells are much higher (Fig. 1a), which may contribute to these discrepancies. This hypothesis is supported by a recent clinical report in which a significant positive association was measured between high levels of PPAR $\gamma$  expression in pancreatic cancer cells and shorter overall survival time.<sup>(18)</sup> Further investigation will be required to better understand the mechanism of PPAR $\gamma$  inhibition of pancreatic cancer cell motility, invasion, and metastasis.

In conclusion, we have demonstrated that inhibition of PPAR $\gamma$  in pancreatic cancer cells decreases cell motility by altering p120ctn localization and suppressing Rac1 and Cdc42 Rho GTPase activities. PPAR $\gamma$  could function as a novel therapeutic target for controlling cancer cell dissemination or metastasis.

## Acknowledgments

We thank Machiko Hiraga and Yuko Satoh for their technical assistance. The present work was supported in part by a Grant-in-Aid for research on the Third Term Comprehensive Control Research for Cancer from the Ministry of Health, Labour and Welfare, Japan to A.N., a grant from the National Institute of Biomedical Innovation to A.N., a grant from the Ministry of Education, Culture, Sports, Science and Technology, Japan (KIBAN-B) to A.N., a grant from the Princess Takamatsu Cancer Research Foundation to A.N., and a grant from the Japanese Human Science Research Foundation to A.N.

- Lefebvre AM, Chen I, Desreumaux P *et al.* Activation of the peroxisome proliferator-activated receptor  $\gamma$  promotes the development of colon tumors in C57BL/6J-APCMin/+ mice. *Nat Med* 1998; **4**: 1053–7.
- Saez E, Tontonoz P, Nelson MC *et al.* Activators of the nuclear receptor PPAR $\gamma$  enhance colon polyp formation. *Nat Med* 1998; **4**: 1058–61.
- Kristiansen G, Jacob J, Buckendahl AC *et al.* Peroxisome proliferator-activated receptor  $\gamma$  is highly expressed in pancreatic cancer and is associated with shorter overall survival times. *Clin Cancer Res* 2006; **12**: 6444–51.
- Masuda T, Wada K, Nakajima A *et al.* Critical role of peroxisome proliferator-activated receptor  $\gamma$  on anoikis and invasion of squamous cell carcinoma. *Clin Cancer Res* 2005; **11**: 4012–21.
- Schaefer KL, Wada K, Takahashi H *et al.* Peroxisome proliferator-activated receptor  $\gamma$  inhibition prevents adhesion to the extracellular matrix and induces anoikis in hepatocellular carcinoma cells. *Cancer Res* 2005; **65**: 2251–9.
- Takahashi H, Fujita K, Fujisawa T *et al.* Inhibition of peroxisome proliferator-activated receptor  $\gamma$  activity in esophageal carcinoma cells results in a drastic decrease of invasive properties. *Cancer Sci* 2006; **97**: 854–60.
- Lea MA, Sura M, Desbordes C. Inhibition of cell proliferation by potential peroxisome proliferator-activated receptor (PPAR)  $\gamma$  agonists and antagonists. *Anticancer Res* 2004; **24**: 2765–71.
- Ramilo G, Valverde I, Lago J, Vieites JM, Cabado AG. Cytotoxic effects of BADGE (bisphenol A diglycidyl ether) and BFDGE (bisphenol F diglycidyl ether) on Caco-2 cells *in vitro*. *Arch Toxicol* 2006; **80**: 748–59.
- Fritz G, Kaina B. Rho GTPases: promising cellular targets for novel anticancer drugs. *Curr Cancer Drug Targets* 2006; **6**: 1–14.
- Taniuchi K, Nakagawa H, Hosokawa M *et al.* Overexpressed P-cadherin/CDH3 promotes motility of pancreatic cancer cells by interacting with p120ctn and activating Rho-family GTPases. *Cancer Res* 2005; **65**: 3092–9.
- Anastasiadis PZ. p120-ctn: a nexus for contextual signaling via Rho GTPases. *Biochim Biophys Acta* 2007; **1773**: 34–46.
- Mosmann T. Rapid colorimetric assay for cellular growth and survival: application to proliferation and cytotoxicity assays. *J Immunol Meth* 1983; **65**: 55–63.
- Yasui N, Sakamoto M, Ochiai A *et al.* Tumor growth and metastasis of human colorectal cancer cell lines in SCID mice resemble clinical metastatic behaviors. *Invasion Metastasis* 1997; **17**: 259–69.
- Nobes CD, Hall A. Rho GTPase control polarity, protrusion, and adhesion during cell movement. *J Cell Biol* 1999; **144**: 1235–44.
- Noren NK, Liu Bp, Burrridge K, Kreft B. p120 catenin regulates the actin cytoskeleton via Rho family GTPase. *J Cell Biol* 2000; **150**: 567–80.
- Nobes CD, Hall A. Rho GTPases control polarity, protrusion, and adhesion during cell movement. *J Cell Biol* 1999; **144**: 1235–44.
- Noren NK, Liu BP, Burrridge K, Kreft B. p120 catenin regulates the actin cytoskeleton via Rho family GTPases. *J Cell Biol* 2000; **150**: 567–80.
- Anastasiadis PZ, Reynolds AB. Regulation of Rho GTPases by p120-catenin. *Curr Opin Cell Biol* 2001; **13**: 604–10.

## Supporting Information

Additional Supporting Information may be found in the online version of this article:

**Fig. S1.** Serum levels of alanine aminotransferase (ALT) in the T0070907-treated metastatic model mice. There was no liver injury at this dose of T0070907.

Please note: Blackwell Publishing are not responsible for the content or functionality of any supporting materials supplied by the authors. Any queries (other than missing material) should be directed to the corresponding author for the article.

# Metformin suppresses intestinal polyp growth in *Apc*<sup>Min/+</sup> mice

Ayako Tomimoto,<sup>1,7</sup> Hiroki Endo,<sup>1,7</sup> Michiko Sugiyama,<sup>1</sup> Toshio Fujisawa,<sup>1</sup> Kunihiro Hosono,<sup>1</sup> Hirokazu Takahashi,<sup>1</sup> Noriko Nakajima,<sup>2</sup> Yoji Nagashima,<sup>3</sup> Koichiro Wada,<sup>4</sup> Hitoshi Nakagama<sup>5</sup> and Atsushi Nakajima<sup>1,6</sup>

<sup>1</sup>Division of Gastroenterology, <sup>2</sup>Department of Molecular Pathology, Yokohama City University School of Medicine, 3-9 Fuku-ura, Kanazawa-ku, Yokohama 236-0004; <sup>3</sup>Department of Pathology, National Institute of Infectious Diseases, 1-23-1 Toyama, Shinjuku-ku, Tokyo 162-8640; <sup>4</sup>Department of Pharmacology, Graduate School of Dentistry, Osaka University, 1-8 Yamadaoka, Suita, Osaka 565-0871; <sup>5</sup>Biochemistry Division, National Cancer Center Research Institute, 1-1 Tsukiji 5-chome, Chuo-ku, Tokyo 104-0045, Japan

(Received June 6, 2008/Revised July 10, 2008/Accepted July 16, 2008/Online publication September 18, 2008)

Metformin is a biguanide derivative that is widely used in the treatment of diabetes mellitus. One of the pharmacological targets of metformin is adenosine monophosphate-activated protein kinase (AMPK). We investigated the effect of metformin on the suppression of intestinal polyp formation in *Apc*<sup>Min/+</sup> mice. Administration of metformin (250 mg/kg) did not reduce the total number of intestinal polyp formations, but significantly reduced the number of intestinal polyp formations larger than 2 mm in diameter in *Apc*<sup>Min/+</sup> mice. To examine the indirect effect of metformin, the index of insulin resistance and serum lipid levels in *Apc*<sup>Min/+</sup> mice were assessed. These factors were not significantly attenuated by the treatment with metformin, indicating that the suppression of polyp growth is not due to the indirect drug action. The levels of tumor cell proliferation as determined by 5-bromodeoxyuridine and proliferating cell nuclear antigen immunohistochemical staining, and apoptosis, via transferase deoxytidyl uridine end labeling staining, in the polyps of metformin-treated mice were not significantly different in comparison to those of control mice. Gene expression of *cyclin D1* and *c-myc* in intestinal polyps were also not significantly different between those two groups. In contrast, metformin activated AMPK in the intestinal polyps, resulting in the inhibition of the activation of mammalian target of rapamycin, which play important roles in the protein synthesis machinery. Metformin suppressed the polyp growth in *Apc*<sup>Min/+</sup> mice, suggesting that it may be a novel candidate as a chemopreventive agent for colorectal cancer. (*Cancer Sci* 2008; 99: 2136–2141)

Colorectal cancer is one of the major causes of mortality.<sup>(1)</sup> Several mechanisms are reported to be involved in the formation of polyps. *Apc*<sup>Min/+</sup> mice, which have a germ-line mutation in the *Apc* tumor suppressor gene<sup>(2)</sup> and have been used extensively for various chemoprevention studies<sup>(3)</sup> are predisposed to the development of multiple adenomas in the small intestine and, to a much lesser extent, in the colon.<sup>(4)</sup> The formation of these polyps is initiated by loss of heterozygosity at the *Apc* locus, which leads to stabilization of the transcription factor  $\beta$ -catenin and constitutive activation of the Wnt signaling pathway, resulting in the expression of target genes, such as *cyclin D1*, *c-myc* and others.<sup>(5)</sup>

Cyclooxygenase-2 (COX-2) is recognized as a potential human colorectal cancer (CRC) chemopreventive target.<sup>(6)</sup> However, recent clinical observations have cast doubt on the vascular safety profile of long-term systemic administration of selective COX-2 inhibitors in humans.<sup>(7)</sup> Therefore, alternative CRC chemoprevention strategies are needed, one of which is to investigate novel therapeutic targets for CRC chemoprevention and another is to minimize the systemic toxicity of COX-2 inhibitors and non-steroidal anti-inflammatory drugs such as aspirin.

Metformin (1, 1-dimethylbiguanide hydrochloride) is one of the biguanide derivatives that has been widely used for a long

time in the treatment of diabetes mellitus.<sup>(8)</sup> The pharmacological action of metformin is reported to be improvement of the insulin resistance in the liver via the activation of adenosine monophosphate-activated protein kinase (AMPK).<sup>(9,10)</sup> Thus, most of the molecular mechanisms involved in metformin action have been studied in liver and adipose tissue in relation to glucose homeostasis and insulin action. However, little is known about the effect of metformin-mediated activation of AMPK in intestinal epithelial cells.

Recently, involvement of the AMPK/mammalian target of rapamycin (mTOR) pathway in the development of various cancers has been reported.<sup>(11,12)</sup> The targets for mTOR signaling are proteins involved in controlling the translational machinery, including the ribosomal protein S6 kinases (S6K) that regulate the initiation and elongation phases of translation.<sup>(13)</sup> With regard to upstream control, mTOR is regulated by signaling pathways linked to several oncoproteins or tumor suppressors, including phosphatidylinositol 3-kinase (PI3K), lipid phosphatase PTEN and AMPK.<sup>(14)</sup> In particular, AMPK activation has been reported to directly inhibit mTOR, resulting in suppression of cell proliferation.<sup>(15)</sup> In addition, it has been demonstrated that growth inhibition of breast cancer cells treated with metformin is associated with the decrease in mTOR and S6 kinase activation *in vitro*.<sup>(16)</sup> The results of the *in vitro* study led us to raise the question whether metformin could act as an anticancer agent for normal and/or transformed intestinal epithelial cells *in vivo*. In this study, we therefore investigated the effect of metformin on the suppression of intestinal polyp growth in *Apc*<sup>Min/+</sup> mice.

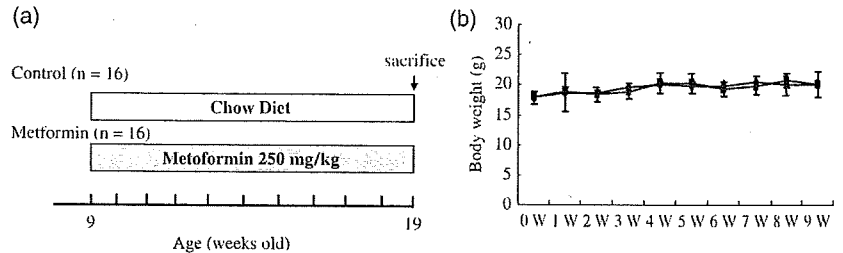
## Materials and Methods

**Animals and reagents.** The mice were treated humanely according to the National Institutes of Health and AERI-BBRI Animal Care and Use Committee guidelines. All animal experiments were approved by the institutional Animal Care and Use Committee of Yokohama City University School of Medicine. C57BL/6-*Apc*<sup>Min/+</sup> mice (*Apc*<sup>Min/+</sup> mice) were purchased from Jackson Laboratory (Bar Harbor, ME, USA). Four to five mice were housed per metallic cage, with sterilized softwood chips as bedding, in a barrier-sustained animal room air-conditioned at 24 ± 2°C and 55% humidity, under a 12-h light : dark cycle.

**Experimental design.** Metformin, which was kindly provided by Dainippon Sumitomo Pharmaceutical (Osaka, Japan), was mixed with a powdered basal diet (Oriental MF, Tokyo, Japan). Nine-week-old *Apc*<sup>Min/+</sup> mice ( $n = 32$ ; 20 for histological analysis, 12 for protein analysis) were divided into two groups: with or without metformin (250 mg/kg per day in the diet) treatment for

<sup>6</sup>To whom correspondence should be addressed. E-mail: nakajima-ky@umin.ac.jp  
<sup>7</sup>These authors contributed equally to this work.

**Fig. 1.** (a) Experimental design for this study. Nine-week-old *Apc<sup>Min/+</sup>* mice ( $n = 32$ ; 20 for histological analysis, 12 for protein or RNA expression analysis) were divided into two groups: with or without metformin (250 mg/kg) treatment for 10 weeks. (b) Mean weights of *Apc<sup>Min/+</sup>* mice in the control and metformin-treated groups. Bodyweight was measured once a week for 10 weeks. No statistically significant differences in bodyweight between metformin-treated and control groups were observed.



10 weeks (Fig. 1). Although the amount of metformin we used in this study is higher than that used in diabetes patients (30–50 mg/kg), previous reports investigating the antidiabetic and antitumor effects of metformin in the mouse model used a higher amount of metformin (250–350 mg/kg) due to the difference of drug sensitivity between rodent and human.<sup>(17–19)</sup> Therefore, we used metformin at the dose of 250 mg/kg in this study.

Bodyweight was measured once a week for 10 weeks. The intestines were collected and filled with 10% neutral-buffered formalin. Number and size of the polyps, as well as their distribution in the intestine, were determined by examination under a stereoscopic microscope.

**Western blot analysis.** The intestinal polyps (>2.5 mm in diameter) were isolated mechanically and the tumor protein was extracted using the T-PER tissue protein extraction reagent (Pierce, Rockford, IL, USA) with 1 mM  $\text{Na}_2\text{VO}_4$ , 25 mM NaF and one tablet of proteinase inhibitor cocktail (Complete Mini; Roche, Basel, Switzerland). Protein concentrations were determined using the Bio-Rad Protein Assay Reagent (Bio-Rad, Richmond, CA, USA). The extracted protein was separated by sodium dodecylsulfate polyacrylamide gel electrophoresis and the separated proteins were transferred onto a PVDF membrane (Amersham, London, UK). The membranes were blocked with 5% bovine serum albumin in Tris-buffered saline and probed with primary antibodies specific for phospho-AMPK $\alpha$ , AMPK $\alpha$ , phospho-mTOR, mTOR, phospho-S6K, S6K (all from Cell Signaling Technology, Danvers, MA, USA) and GAPDH (Trevigen, Gaithersburg, MD, USA). Horseradish peroxidase-conjugated secondary antibodies and the ECL detection kit (Amersham) were used for the detection of specific proteins. The results were normalized to the signal generated from GAPDH.

Five polyps per mouse were analyzed by western blotting (a total of 30 polyps from each group) and representative images are demonstrated.

**Gene expression analysis.** Total RNA was extracted from the polyps using the RNeasy Mini Kit (Qiagen, Hilden, Germany). For real-time reverse transcription polymerase chain reaction, total RNA was reverse-transcribed into cDNA and amplified by real-time quantitative polymerase chain reaction using the ABI PRISM 7700 System (Applied Biosystems, Foster City CA, USA). Probes and primer pairs specific for *cyclin D1*, *c-myc* and  $\beta$ -actin were purchased from Applied Biosystems. The concentrations of the target genes were determined using the competitive computed tomography method and values were normalized to the internal control. Ten polyps (>2.0 mm in diameter) from each group were analyzed.

**Histological analyses.** Paraffin-embedded sections were deparaffinized and subjected to hematoxylin–eosin staining and immunohistochemistry for  $\beta$ -catenin using Histofine simple stain mouse max PO kit (Nichirei Laboratories, Tokyo, Japan) in accordance with the manufacturer's instructions. The primary  $\beta$ -catenin antibody (BD Transduction Laboratories, San Diego, CA, USA) was diluted 1:2000 and nuclear counterstaining was performed with hematoxylin. Isotype-matched immunoglobulin was used as a control to determine the non-specific staining. Three polyps from each mice were randomly selected and

stained with  $\beta$ -catenin (a total of 60 polyps were analyzed). The expression of  $\beta$ -catenin detected via immunohistochemistry was quantitated by the scoring index according to Jawhari *et al.* and Oka *et al.*<sup>(20,21)</sup> All the histological findings were judged blind by two independent pathologists (N. N. and Y. N.).

**Cell proliferation assay.** We evaluated the 5-bromodeoxyuridine (BrdU) labeling index to determine the proliferative activity of the tumor cells. BrdU (BD Biosciences, Franklin Lakes, NJ, USA) was used to label the tumor cells undergoing DNA replication. It was diluted in phosphate-buffered saline at 1 mg/mL and 1 mg of BrdU solution was injected i.p. into mice 1 h prior to the killing of the mice. Immunohistochemical detection of BrdU was performed using a commercial kit (BD Biosciences). The BrdU labeling index was expressed as the percentage of cells showing positive staining for BrdU relative to the total number of cells. At least three to five representative areas in a section were selected by light-microscopic examination at 400-fold magnification and 1000–2000 tumor cells were counted as described previously.<sup>(22)</sup> Three polyps (>2.0 mm in diameter) from each mouse were randomly selected and counted (a total of 60 polyps were analyzed). The counting of BrdU-positive tumor cells in the polyp sections was repeated in triplicate and assessed blindly to reduce the bias in the results. Proliferation cell nuclear antigen (PCNA) was also used to label tumor cells undergoing DNA replication and the immunohistochemical detection of PCNA was performed using a commercial kit (Zymed Laboratories, South San Francisco CA, USA). The PCNA labeling index was determined identically as the BrdU index. The apoptotic tumor cells were stained using a transferase deoxytidyl uridine end labeling (TUNEL) staining kit according to the manufacturer's instruction (Wako Pure Chemical, Tokyo). The apoptotic index, which was expressed as the percentage of cells showing positive TUNEL staining relative to the total number of cells, was determined identically as the BrdU index.

**Plasma lipid levels and insulin resistance.** The levels of plasma triglycerides, cholesterol, insulin and glucose were measured using a WAKO enzyme-linked immunosorbent assay (ELISA) kit ( $n = 10$  from each group). Metformin is widely used as an antidiabetic drug to improve insulin resistance. Therefore, the status of insulin resistance as represented by homeostasis model assessment of insulin resistance (HOMA-IR) was investigated. HOMA-IR is calculated using the following formula:  $\text{HOMA-IR} = \text{fasting plasma immunoreactive insulin (IRI; } \mu\text{U/mL)} \times \text{fasting plasma glucose (FBG; mg/dL)} / 405$ . We also measured the plasma concentration of triglycerides and cholesterol according to the manufacturer's instructions.

**Statistical analyses.** Statistical analysis for the blood tests was conducted using the Mann–Whitney *U*-test. Other statistical analyses were performed using the Student's *t*-test. Differences were considered significant at  $P < 0.05$ .

## Results

**Suppression of intestinal polyp growth by metformin in *Apc<sup>Min/+</sup>* mice.** It has been reported that the majority of polyps are located in the small intestine in *Apc<sup>Min/+</sup>* mice.<sup>(23)</sup> The total number of

Table 1. Effect of metformin on the formation of polyps in *Apc<sup>Min/+</sup>* mice

Diet	No. of mice	No. of polyp/mouse	Average size of polyps (mm)	No. of polyps >2 mm
Control	10	42.11 ± 4.76	1.935 ± 0.028	19.44 ± 3.87
Metformin	10	38.22 ± 4.53	1.648 ± 0.026*	8.44 ± 2.38**

Mean ± standard error significantly different from the basal diet group at \**P* = 0.039; \*\**P* = 0.019.

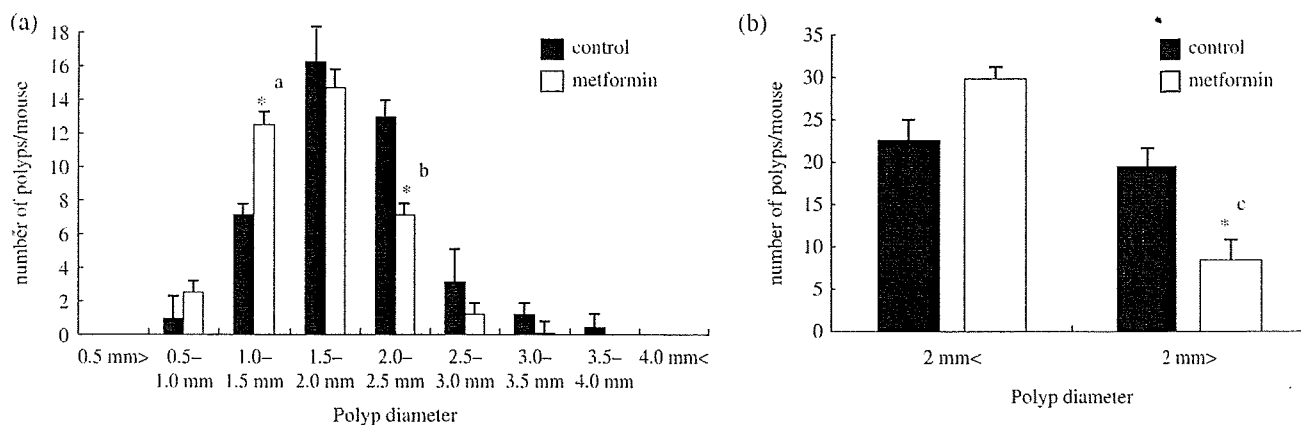


Fig. 2. Effect of metformin on the number and the size distribution of intestinal polyps in *Apc<sup>Min/+</sup>* mice. *Apc<sup>Min/+</sup>* mice were fed either a basal diet or a diet containing metformin (250 mg/kg) for 10 weeks. (a) The number of polyps per mouse in each size class is given as a mean value. (b) Comparison of polyp size below 2 mm and over 2 mm in diameter. Bars represent standard error. \*\**P* = 0.034; \**P* = 0.032; \**P* = 0.019.

polyps in the small intestine was not significantly different between the control and metformin-treated groups (Table 1). Therefore, the size distribution of intestinal polyps was investigated (Fig. 2a). Interestingly, the number of polyps ranging 1.0–1.5 mm in diameter was significantly increased and the number of polyps ranging 2.0–2.5 mm in diameter was significantly decreased with metformin treatment compared with the control (Fig. 2a). Therefore, we found that treatment with metformin significantly reduced the number of polyps larger than 2.0 mm in diameter (Fig. 2b). These results indicate that metformin reduced the size, but did not decrease the total number of intestinal polyps, suggesting that metformin may inhibit the growth of polyps.

**Effect of metformin on proliferation of intestinal tumor cells.** There was no histological difference observed in hematoxylin–eosin stained polyps between control and metformin-treated *Apc<sup>Min/+</sup>* mice. In addition, no difference in the immunohistochemical staining pattern of  $\beta$ -catenin in tumor tissues was observed between the control and metformin-treated groups (Fig. 3a). There were also no significant differences in the pathological scoring indices of  $\beta$ -catenin immunohistochemical staining in tumor cells between control and metformin-treated groups (data not shown). The BrdU index of the intestinal polyps (>2 mm in diameter) in the metformin-treated group was slightly decreased compared with the control group, but was not significantly different (*n* = 60, Fig. 3b). The same result was obtained by investigating the PCNA index (*n* = 52, Fig. 3c). The percentage of apoptotic cells in tumor tissues, investigated by TUNEL staining, was not significantly altered in the metformin-treated group as compared to the control group (*n* = 48, Fig. 3d). These results suggest that metformin suppresses the intestinal polyp growth in *Apc<sup>Min/+</sup>* mice neither through the significant inhibition of tumor cell proliferation nor through upregulation of apoptosis in tumor cells. To confirm these results, the gene expression analyses of *cyclin D1* and *c-myc* were performed, and no difference in the gene expression was detected in polyps of control and metformin-treated groups (*n* = 20, Fig. 3e).

**Effect of metformin on plasma lipid levels and insulin resistance.** Metformin is widely used as an antidiabetic drug that improves insulin resistance for patients with diabetes mellitus. Therefore, we investigated the effect of metformin on plasma lipid levels and insulin resistance. There was no significant difference in plasma triglyceride and cholesterol levels between the control and metformin-treated groups at our experimental dosages (Fig. 4). In addition, blood glucose levels and insulin resistance, represented by HOMA-IR, between the control and metformin-treated groups were similar (Figs 4c,d). Furthermore, bodyweights between the two groups were similar (Fig. 1b). Because *Apc<sup>Min/+</sup>* mice are not a diabetic model, it is reasonable that marked alterations were not observed in our experimental condition.

**Metformin-mediated activation of AMPK inhibits the mTOR/S6K pathway in intestinal polyps.** Western blotting showed abundant expression of AMPK in the intestine and colon as compared to the liver (Fig. 5e). It is speculated that one of the pharmacological targets of metformin is AMPK,<sup>(10)</sup> which has been reported to inhibit the mTOR/S6K signaling pathway.<sup>(15)</sup> Therefore, we hypothesized that metformin could inhibit the mTOR/S6K signaling pathway through activation of AMPK, resulting in downregulation of the protein synthesis machinery in the intestinal polyps. Western blot analysis revealed that the treatment with metformin stimulated AMPK phosphorylation in the intestinal polyps (Fig. 5a). Further, phosphorylation of mTOR and S6K proteins was significantly inhibited by the treatment with metformin (Fig. 5b–d). These results indicate that the treatment with metformin inhibits the mTOR/S6K/S6 signaling pathway, which may lead to the suppression of protein synthesis machinery in carcinogenesis.

## Discussion

In the present study, we clearly showed that metformin suppressed intestinal polyp growth in *Apc<sup>Min/+</sup>* mice, the first report regarding the inhibition of *in vivo* polyp growth by metformin.

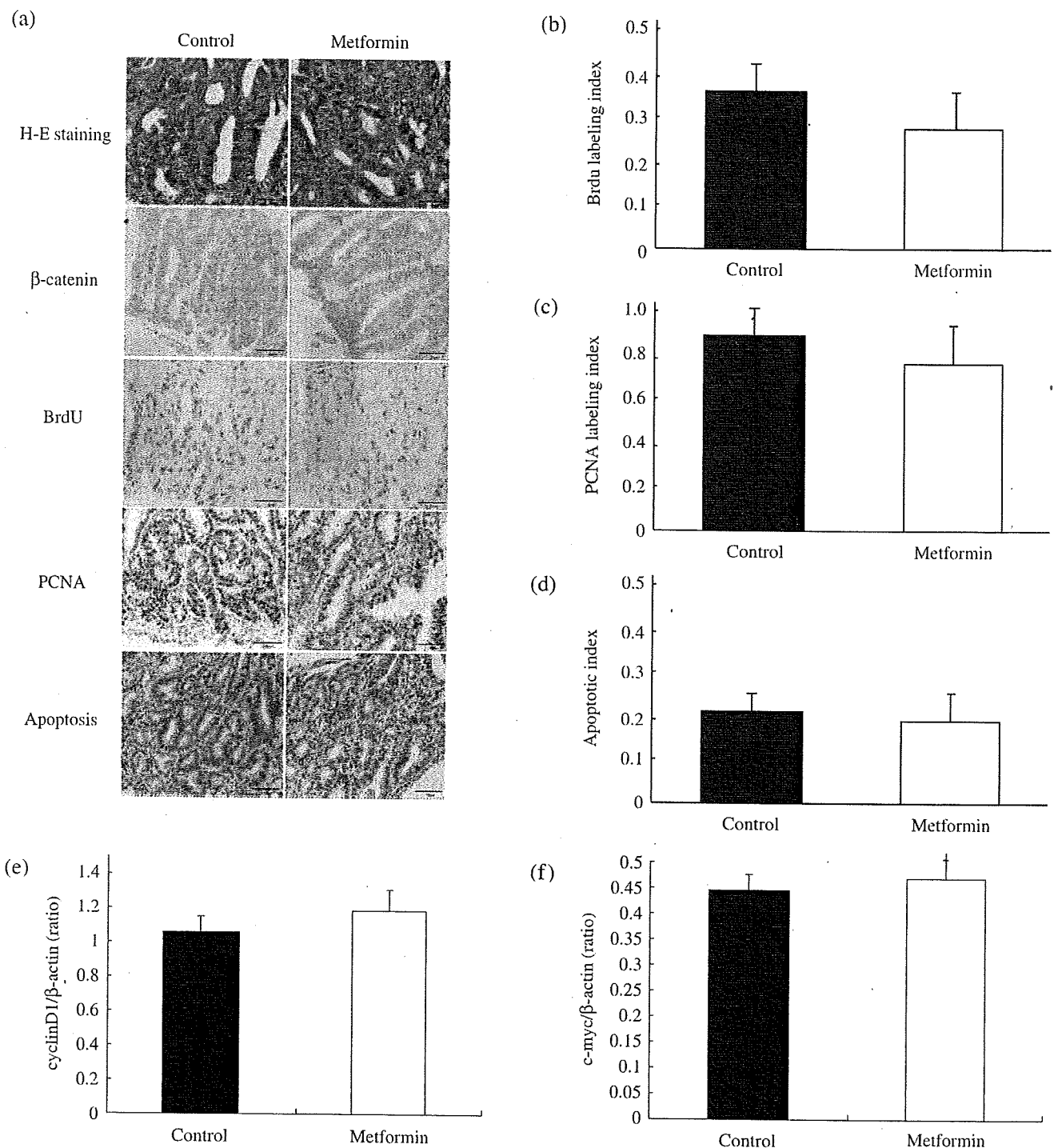


**Fig. 3.** Immunohistochemistry for  $\beta$ -catenin, cell proliferation assay using 5-bromodeoxyuridine (BrdU) and proliferating cell nuclear antigen (PCNA), apoptosis assay, and gene expression analyses of *cyclin D1* and *c-myc* in the tumor cells. (a) HE staining and immunohistochemical staining for  $\beta$ -catenin, BrdU and PCNA in intestinal tumors from *Apc<sup>Min/+</sup>* mice fed a basal diet or treated with metformin. Transferase deoxytidyl uridine end labeling staining in tumors are also demonstrated. (b,c,d) Calculations for the BrdU, PCNA and apoptotic indices are detailed in Materials and Methods section. No significant difference was observed in each index category between metformin-treated and control groups. Gene expression of (e) *cyclin D1* and (f) *c-myc* in intestinal polyps using real time reverse transcription polymerase chain reaction analysis are also shown.  $\beta$ -Actin was used as the internal control. No significant difference was observed in these gene expression levels between metformin-treated and control groups. Bars represent standard error.

Metformin is widely used as an antidiabetic drug that improves insulin resistance. Therefore, we investigated the effect of metformin on serum lipid levels and insulin resistance in order to determine the indirect effects of this drug. Our results

demonstrated that metformin did not attenuate the blood glucose, HOMA-IR and plasma lipid levels in *Apc<sup>Min/+</sup>* mice, indicating that the suppression of polyp growth was due to some direct effects other than attenuation of insulin resistance or hyperlipidemia. In

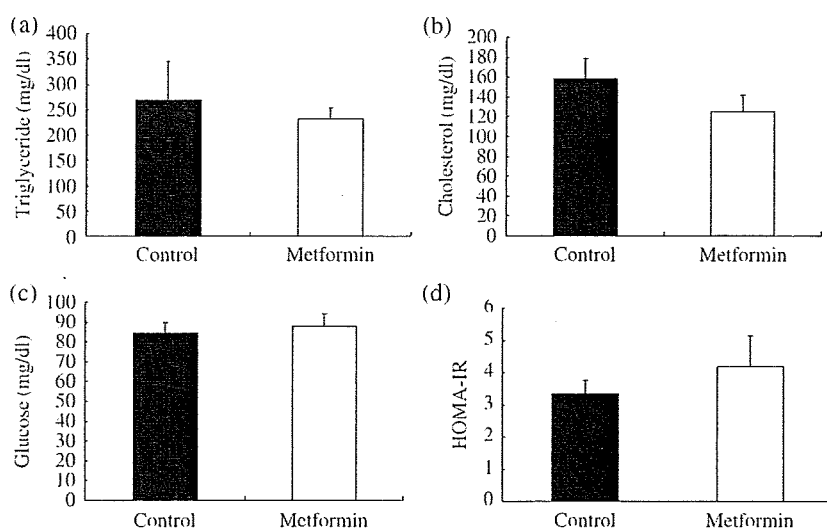


Fig. 4. Plasma levels of insulin, triglyceride, cholesterol and glucose. *Apc<sup>Min/+</sup>* mice were fed a basal diet (control) or a diet containing metformin (250 mg/kg). Plasma and blood were obtained after 12 h fasting. (a) Cholesterol, (b) triglyceride, (c) insulin, (d) blood glucose and (e) homeostasis model assessment of insulin resistance (HOMA-IR) levels are shown. HOMA-IR was used to calculate insulin resistance using the following formula: HOMA-IR = fasting plasma immunoreactive insulin (IRI;  $\mu\text{U/mL}$ )  $\times$  fasting plasma glucose (FBG; mg/dL)/405. No statistical significance was observed in the plasma levels of cholesterol, triglyceride and HOMA-IR between metformin-treated and control groups. Bars represent standard error.

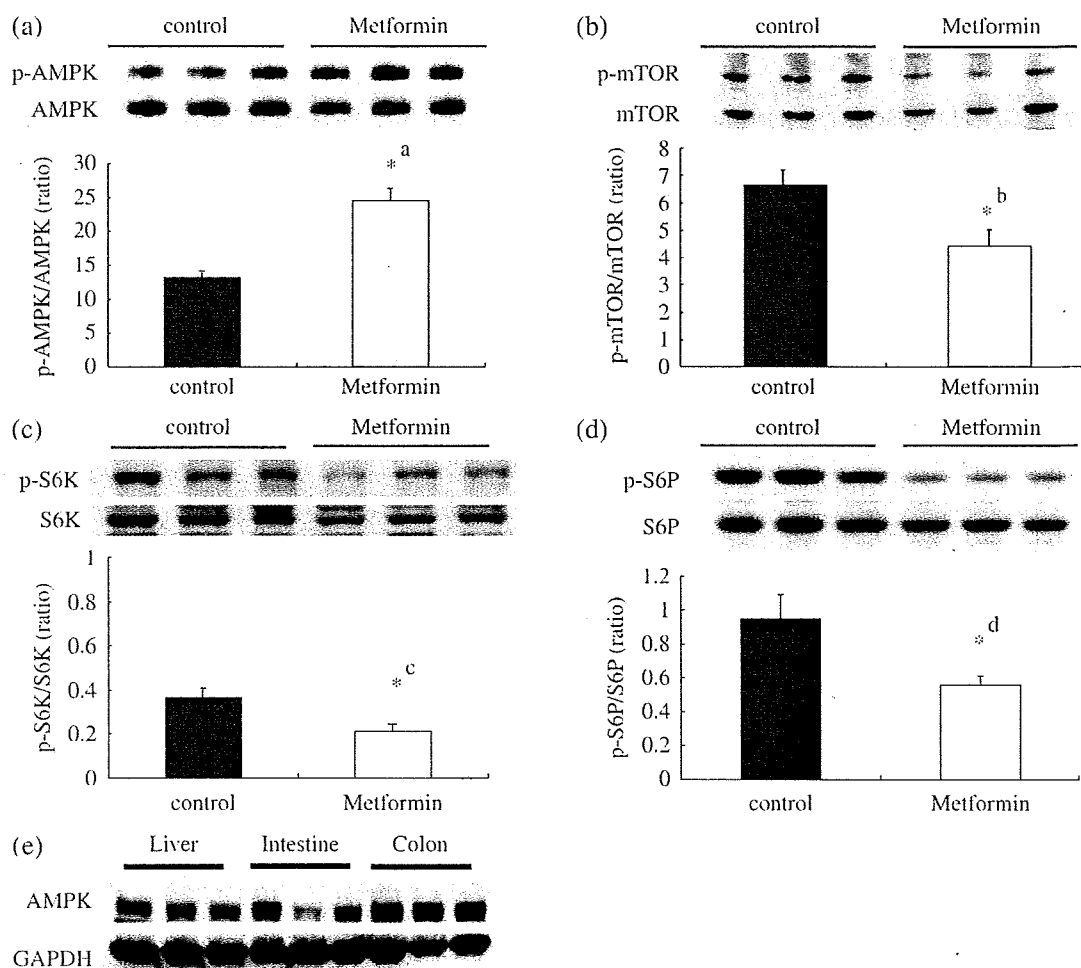


Fig. 5. Treatment with metformin activates adenosine monophosphate-activated protein kinase (AMPK) and downregulates the mammalian target of rapamycin (mTOR)/S6K pathway. *Apc<sup>Min/+</sup>* mice were treated with a basal diet (control,  $n = 6$ ) and a diet containing metformin (250 mg/kg,  $n = 6$ ) for 10 weeks. Western blotting was performed using intestinal tumors (>2 mm in diameter) from both groups; five polyps from each mice were analyzed (a total of 60 polyps were assessed). Representative western blotting images are demonstrated. (a) Immunoblotting using antibodies against phosphorylated AMPK and total AMPK. The relative activity of phosphorylated AMPK against total AMPK is demonstrated. (b) Phospho-mTOR, mTOR and relative activity of mTOR. (c) Phospho-S6K/S6. (d) Phospho-p70 protein S6 (S6P)/total S6. (e) Western blotting analysis of the expression of AMPK in small intestine, colon and liver from *Apc<sup>Min/+</sup>* mice. glyceraldehyde 3-phosphate dehydrogenase (GAPDH) is shown as a loading control. Bars represent standard error. \*\* $P = 0.0016$ ; \* $P = 0.0009$ ; \* $P = 0.0103$ ; \* $P = 0.0054$ .

fact, *Apc*<sup>Min/+</sup> mice are not a diabetic model, so it is understandable that metformin did not decrease the blood glucose level. Furthermore, according to the published work, no hypoglycemic side-effects have been reported to date for metformin, whereas side-effects are known for other antidiabetic drugs, such as sulfonylurea, and no reports show that metformin has any therapeutic effect on hyperlipidemia.<sup>(24)</sup> Therefore, our results are compatible with these previous clinical studies in that metformin did not attenuate the blood glucose, HOMA-IR and plasma lipid levels in *Apc*<sup>Min/+</sup> mice.

To examine the direct effect of metformin with regard to the growth inhibition of intestinal polyps, we analyzed the tumor cell proliferation by BrdU and PCNA immunostainings. Both BrdU and PCNA indices were decreased slightly, but not significantly by the metformin treatment. In addition to these results, the apoptotic cell index was also not altered by the treatment with metformin. Nuclear translocated  $\beta$ -catenin plays an important role as a major transcription factor in regulation of tumor cell proliferation. In this study, we examined the immunohistochemical staining of  $\beta$ -catenin in tumor tissues and found no difference in staining pattern between metformin-treated and control polyps. These results were confirmed by the findings showing no difference in expression levels of cyclin D1 and c-myc, which are the downstream genes of  $\beta$ -catenin.

On the contrary, one of the known pharmacological actions of metformin is activation of AMPK.<sup>(10)</sup> In addition, activation of AMPK has been reported to inhibit the mTOR signaling pathway.<sup>(15)</sup> Therefore, we investigated whether metformin-mediated activation of AMPK could be involved in the suppression of polyp growth *in vivo*. Our data suggested that metformin-activated AMPK,

resulting in the inhibition of mTOR and S6K protein activation. Because the mTOR signaling pathway is known to play important roles in the protein synthesis machinery, inhibition of the mTOR pathway by metformin-mediated activation of AMPK may be one of the direct mechanisms to suppress polyp growth *in vivo*. There is abundant intestinal expression of AMPK, therefore the activation of AMPK by drugs, such as metformin, may be a novel therapeutic strategy in the chemoprevention of colorectal cancer. We present here only a proposed mechanism, further study will be necessary to elucidate the precise mechanisms underlying the suppressive effects of tumor growth mediated by such drugs.

In conclusion, metformin suppressed intestinal polyp growth in *Apc*<sup>Min/+</sup> mice, potentially through the activation of AMPK, resulting in the inhibition of the mTOR/S6K signaling pathway and subsequent inhibition of the protein synthesis machinery. Further studies are needed to elucidate the precise mechanisms underlying inhibition of polyp growth by metformin. Metformin is a novel candidate for colon cancer chemoprevention.

### Acknowledgments

We thank Machiko Hiraga for her technical assistance. This work was supported in part by a Grant-in-Aid for research on the Third Term Comprehensive Control Research for Cancer from the Ministry of Health, Labor and Welfare, Japan, to A. N., a grant from the National Institute of Biomedical Innovation (NBIO) to A. N., a grant from the Ministry of Education, Culture, Sports, Science and Technology, Japan (KIBAN-B), to A. N., and a research grant of the Princess Takamatsu Cancer Research Fund to A. N.

### References

- Jemal A, Tiwari RC, Murray T *et al*. American Cancer Society. Cancer statistics, 2004. *CA Cancer J Clin* 2004; **54**: 8–29.
- Moser AR, Pitot HC, Dove WF. A dominant mutation that predisposes to multiple intestinal neoplasia in the mouse. *Science* 1990; **247**: 322–4.
- Corpet DE, Pierre F. Point: from animal models to prevention of colon cancer. Systematic review of chemoprevention in min mice and choice of the model system. *Cancer Epidemiol Biomarkers Prev* 2003; **12**: 391–400.
- Su LK, Kinzler KW, Vogelstein B *et al*. Multiple intestinal neoplasia caused by a mutation in the murine homolog of the APC gene. *Science* 1992; **256**: 668–70.
- He TC, Sparks AB, Rago C *et al*. Identification of c-MYC as a target of the APC pathway. *Science* 1998; **281**: 1509–12.
- Gupta RA, Dubois RN. Colorectal cancer prevention and treatment by inhibition of cyclooxygenase-2. *Nat Rev Cancer* 2001; **1**: 11–21.
- Psaty BM, Furberg CD. COX-2 inhibitors – lessons in drug safety. *N Engl J Med* 2005; **352**: 1133–5.
- Witters LA. The blooming of the French lilac. *J Clin Invest* 2001; **108**: 1105–7.
- Shaw RJ, Lamia KA, Vasquez D *et al*. The kinase LKB1 mediates glucose homeostasis in liver and therapeutic effects of metformin. *Science* 2005; **310**: 1642–6.
- Zhou G, Myers R, Li Y *et al*. Role of AMP-activated protein kinase in mechanism of metformin action. *J Clin Invest* 2001; **108**: 1167–74.
- Carretero J, Medina PP, Blanco R *et al*. Dysfunctional AMPK activity, signaling through mTOR and survival in response to energetic stress in LKB1-deficient lung cancer. *Oncogene* 2007; **26**: 1616–25.
- Motoshima H, Goldstein BJ, Igata M, Araki E. AMPK and cell proliferation – AMPK as a therapeutic target for atherosclerosis and cancer. *J Physiol* 2006; **574**: 63–71.
- Mamane Y, Petroulakis E, LeBacquer O, Sonenberg N. mTOR, translation initiation and cancer. *Oncogene* 2006; **25**: 6416–22.
- Hay N. The Akt-mTOR tango and its relevance to cancer. *Cancer Cell* 2005; **8**: 179–83.
- Martin DE, Hall MN. The expanding TOR signaling network. *Curr Opin Cell Biol* 2005; **17**: 158–66.
- Zakikhani M, Dowling R, Fantus IG, Sonenberg N, Pollak M. Metformin is an AMP kinase-dependent growth inhibitor for breast cancer cells. *Cancer Res* 2006; **66**: 10269–73.
- Bergheim I, Guo L, Davis MA *et al*. Metformin prevents alcohol-induced liver injury in the mouse: critical role of plasminogen activator inhibitor-1. *Gastroenterology* 2006; **130**: 2099–112.
- Buzzai M, Jones RG, Amaravadi RK *et al*. Systemic treatment with the antidiabetic drug metformin selectively impairs p53-deficient tumor cell growth. *Cancer Res* 2007; **67**: 6745–52.
- Zou MH, Kirkpatrick SS, Davis BJ *et al*. Activation of the AMP-activated protein kinase by the anti-diabetic drug metformin *in vivo*. *J Biol Chem* 2004; **279**: 43940–51.
- Jawhari A, Jordan S, Poole S, Browne P, Pignatelli M, Farthing MJ. Abnormal immunoreactivity of the E-cadherin-catenin complex in gastric carcinoma: relationship with patient survival. *Gastroenterology* 1997; **112**: 46–54.
- Oka H, Shiozaki H, Kobayashi K *et al*. Expression of E-cadherin cell adhesion molecules in human breast cancer tissues and its relationship to metastasis. *Cancer Res* 1993; **53**: 1696–701.
- William HG, Dan HM, Britt-Marie L. The prognostic value of proliferation indices: a study with *in vivo* bromodeoxyuridine and Ki-67. *Breast Cancer Res Treatment* 2000; **59**: 113–23.
- Yamada Y, Hata K, Hirose Y *et al*. Microadenomatous lesions involving loss of *Apc* heterozygosity in the colon of adult *Apc* (Min/+) mice. *Cancer Res* 2002; **62**: 6367–70.
- Stumvoll M, Nurbhan N, Perriello G, Dailey G, Gerich JE. Metabolic effects of metformin in non-insulin-dependent diabetes mellitus. *N Engl J Med* 1995; **333**: 550–4.



## Expression of adiponectin receptors, AdipoR1 and AdipoR2, in normal colon epithelium and colon cancer tissue

KYOKO YONEDA<sup>1</sup>, \*AYAKO TOMIMOTO<sup>1</sup>, HIROKI ENDO<sup>1</sup>, HIROSHI IIDA<sup>1</sup>, MICHIKO SUGIYAMA<sup>1</sup>, HIROKAZU TAKAHASHI<sup>1</sup>, HIRONORI MAWATARI<sup>1</sup>, YUICHI NOZAKI<sup>1</sup>, KOJI FUJITA<sup>1</sup>, MASATO YONEDA<sup>1</sup>, MASAHIKO INAMORI<sup>1</sup>, NORIKO NAKAJIMA<sup>2</sup>, KOICHIRO WADA<sup>3</sup>, YOJI NAGASHIMA<sup>4</sup>, HITOSHI NAKAGAMA<sup>5</sup>, HIROSHI UOZAKI<sup>6</sup>, MASASHI FUKAYAMA<sup>6</sup> and ATSUSHI NAKAJIMA<sup>1</sup>

<sup>1</sup>Gastroenterology Division, Yokohama City University School of Medicine, 3-9 Fuku-ura, Kanazawa-ku, Yokohama;

<sup>2</sup>Department of Pathology, National Institute of Infectious Diseases, 1-23-1 Toyama, Shinjuku-ku, Tokyo;

<sup>3</sup>Department of Pharmacology, Graduate School of Dentistry, Osaka University, 1-8 Yamadaoka, Suita, Osaka;

<sup>4</sup>Department of Molecular Pathology, Yokohama City University School of Medicine, 3-9 Fuku-ura, Kanazawa-ku, Yokohama;

<sup>5</sup>Biochemistry Division, National Cancer Center Research Institute, 1-1 Tsukiji 5-chome, Chuo-ku, Tokyo;

<sup>6</sup>Department of Pathology, Graduate School of Medicine, The University of Tokyo, 7-3-1 Hongo, Bunkyo-ku, Tokyo, Japan

Received March 20, 2008; Accepted May 2, 2008

DOI: 10.3892/or\_00000031

**Abstract.** Adiponectin is secreted by adipocytes and is a key hormone responsible for insulin sensitization. Recent studies have shown that plasma adiponectin is decreased in patients with breast, endometrial and gastric cancer. However, the effect of adiponectin on colorectal carcinogenesis is controversial. It is now well known that the adiponectin receptor exists in two isoforms, adiponectin receptor 1 (AdipoR1) and adiponectin receptor 2 (AdipoR2). We examined the expression of the adiponectin receptors on normal colon mucosa and colon cancer tissues in a human study using real-time RT-PCR, Western blotting and immunohistochemical staining. Adiponectin receptors, AdipoR1/AdipoR2, were expressed in normal colon epithelial and colon cancer cells. Furthermore, laser microdissection was performed to confirm our results. These results suggest that adiponectin may exert some effects on normal colon epithelium or colon cancer cells directly through adiponectin receptors. Further studies are required to elucidate the function of the AdipoRs activated by adiponectin and the downstream mechanisms of AdipoRs in colon cancer cells.

### Introduction

Adipose tissue secretes several bioactive substances known as adipocytokines and obesity is an important risk factor for

many diseases, including diabetes mellitus (DM) (1,2). Human adiponectin, earlier known as ACRP30 or AdipoQ, is a 30 kDa adipokine composed of 247 amino acids, which is encoded by the *apM1* gene and is located on chromosome 3, locus 3q27 (3-5). Adiponectin is secreted by adipocytes and is a key hormone responsible for insulin sensitization. While the adiponectin protein is abundantly found in the plasma of healthy human subjects, its plasma levels are dramatically decreased in patients with obesity and/or type 2 DM (2,3,6). Since obesity and type 2 DM have been reported to be associated with an elevated risk of colorectal cancer (CRC) (7), it has been speculated that the plasma level of adiponectin may be related to the risk of CRC. Furthermore, previous studies have shown that decreased levels of plasma adiponectin were observed in patients with breast, endometrial and gastric cancer (8-11). However, several contradictory results have been reported from human clinical studies on the relationship between the plasma levels of adiponectin and the risk of CRC (12,13). It is now well known that the adiponectin receptor exists in two isoforms; adiponectin receptor 1 (AdipoR1), which is abundantly expressed in the skeletal muscle and adiponectin receptor 2 (AdipoR2), which is predominantly expressed in the liver (14). Recent studies have shown that the adiponectin receptors are expressed in human breast (15) and prostate cancer (16). Takahata *et al* showed that AdipoR1 and AdipoR2 (AdipoRs) were expressed in normal breast epithelial cells and breast cancer cells (15). However, it remains unclear whether the adiponectin receptors are also expressed in the normal colon mucosa and colon cancer tissue. In this study, we examined at genetic and protein expression levels the expression of AdipoRs on normal colon mucosa and colon cancer tissues from patients.

*Correspondence to:* Dr Atsushi Nakajima, Gastroenterology Division, Yokohama City University School of Medicine, 3-9 Fuku-ura, Kanazawa-ku, Yokohama, Japan  
E-mail: nakajima-ky@umin.ac.jp

*Key words:* colon cancer, adiponectin, adiponectin receptor

### Materials and methods

*Patients.* We evaluated patients with CRC and normal subjects who underwent colonoscopy at Yokohama City University

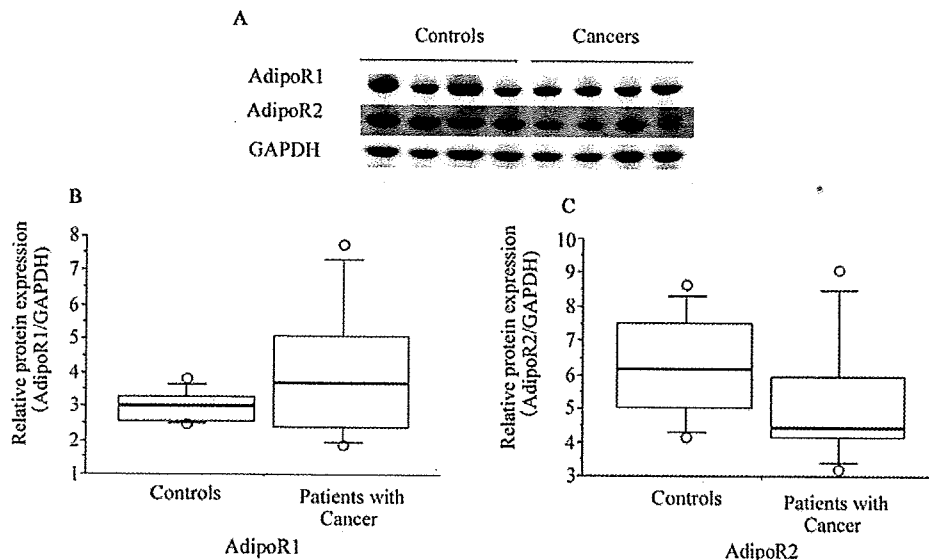


Figure 1. (A) The protein expression levels of AdipoR1 and AdipoR2 were examined with Western blotting. (B and C) Box plots showing interquartile range (box), median (thick line), range (thin line) and outliers (circles). Values are normalized to the level of GAPDH as the internal control. AdipoR1 (B) and AdipoR2 (C) in patients with cancer and control subjects. All samples expressed the AdipoR1 and AdipoR2 proteins, with no significant difference seen in these levels between the control and cancer specimens.

Hospital from April to September 2007 after informed consent was provided. A total of 34 cases were studied. CRC was diagnosed by histological analysis. The study was conducted with the approval of the Ethics Committee of Yokohama City University.

**Western blotting.** Biopsy specimens were homogenized and resolved by polyacrylamide gel (Bio-Rad Japan, Tokyo, Japan). Proteins were transferred onto a Hybond-P PVDF transfer membrane (Amersham Biosciences, Little Chalfont, UK) and incubated with antibodies to AdipoR1 (1:2000) or AdipoR2 (1:1000, Santa Cruz Biotechnology, Santa Cruz, CA, USA) as primary antibodies. For the internal control, membranes were incubated with an antibody to GAPDH (1:1000, Trevigen, Gaithersburg, MD, USA) as the primary antibody. Immune complexes were detected with the ECL Western blot system (Amersham Biosciences).

**Real-time reverse transcriptase-polymerase chain reaction (real-time RT-PCR).** Total RNA from the biopsy specimens was purified using an RNeasy kit (Qiagen, Hilden, Germany). Real-time RT-PCR was carried out using Taq Man reverse transcription reagents and Taq Man gene expression master mix (Applied Biosystems). The primers were AdipoR1, AdipoR2 and  $\beta$ -actin (Applied Biosystems). The expression levels of *AdipoR1* and *AdipoR2* were shown as a ratio to  $\beta$ -actin as the internal control. To compare the results achieved in colon RNA with liver and skeletal muscle mRNA, human liver total RNA and human skeletal muscle total RNA (Clontech Laboratories, Mountain View, CA, USA) were also evaluated using real-time RT-PCR.

**Laser microdissection and real-time RT-PCR.** Frozen biopsy specimens were cut into 7- $\mu$ m sections and stained with toluidine blue (Muto Pure Chemicals, Tokyo, Japan). The cancer cells and normal cells were collected with PALM

MicroLaser Systems (P.A.L.M. Microlaser Technologies, Bernried, Germany). Total RNA was purified using an RNAqueous-micro kit (Applied Biosystems). The real-time RT-PCR procedure was performed as described above.

**Immunohistochemical staining.** Formalin-fixed and paraffin-embedded samples were deparaffinized and rehydrated. The sections were incubated with antibodies to AdipoR1 (1:400) and AdipoR2 (1:400, Phoenix Pharmaceuticals) as the primary antibodies using an LSAB2 kit (Dako cytometry). The sections were incubated with biotinylated immunoglobulin as the secondary antigen and were then treated with peroxidase-conjugated streptavidin. The antibody complex was visualized with 3,3'-diaminobenzidine, tetrahydrochloride (Dojindo Laboratories, Kumamoto, Japan).

**Statistical analysis.** The statistical analyses were performed with StatView-J 5.0 (SAS Institute, Cary, NJ, USA). The association between the clinicopathological factors and expression levels of the AdipoRs was assessed with the Student's t-test. P-values of <0.05 were considered significant.

## Results

**Patients.** The characteristics of the CRC patients and control subjects are shown in Table I. The CRC patients (n=16) and control subjects (n=18) were similar with regard to age and body mass index (BMI). Patients using drugs which could influence serum adiponectin levels and patients with inflammatory bowel diseases were excluded from the present study.

**Western blotting of AdipoR1 and AdipoR2.** We examined the protein expression levels of AdipoRs using Western blotting (Fig. 1). The expression levels of the AdipoRs were detected in the controls and colon cancer tissues (Fig. 1A). All samples

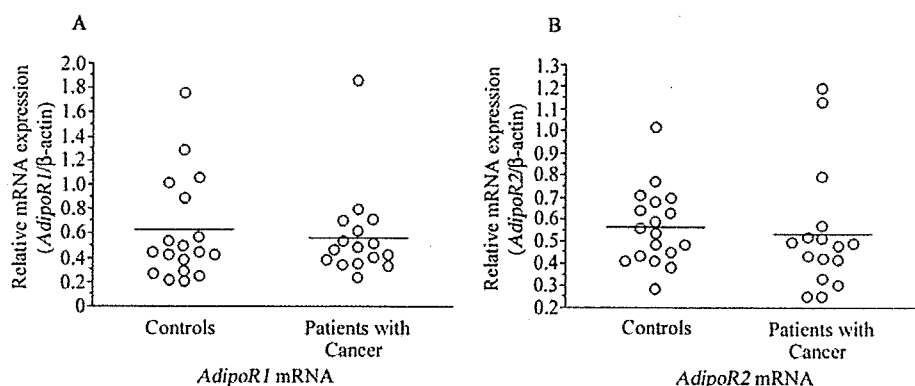


Figure 2. Colonic mRNA expression levels of *AdipoR1* (A) and *AdipoR2* (B) in patients with cancer and control subjects were evaluated using real-time RT-PCR. Values are normalized to the level of  $\beta$ -actin. Bar, mean value of patients with cancer and control subjects. All samples expressed *AdipoR1* and *AdipoR2* mRNA, the expression levels of which were not significantly different between the control and cancer specimens.

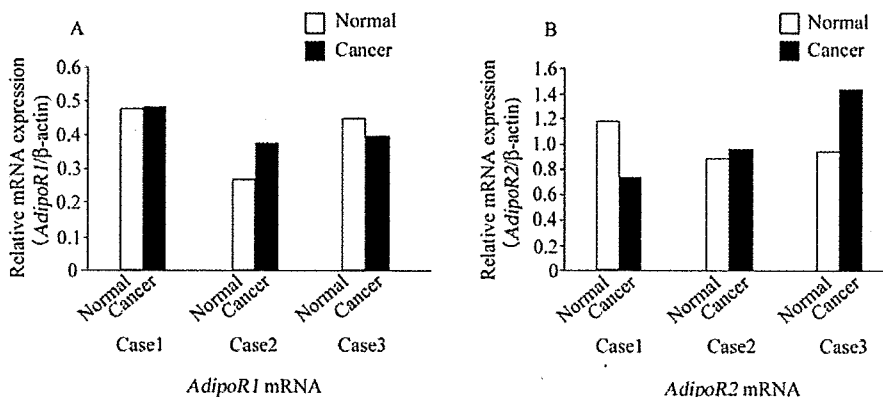


Figure 3. *AdipoR1* (A) and *AdipoR2* (B) mRNA expression levels of colonic epithelial cells and cancer cells collected from patients with cancer were examined with a laser microdissection system. Real-time RT-PCR was carried out. Values are normalized to the level of  $\beta$ -actin. All cell samples expressed *AdipoR1* mRNA and *AdipoR2* mRNA, the levels of expression of which were not significantly different between the normal cells and cancer cells.

Table I. Characteristics of cancer patients and control subjects.

	Controls	Patients with cancer	P-value
Number	18	16	
Location of cancer		C=1, A=2, T=1, S=7, R=5	
Age (years)	59.89 $\pm$ 2.4	63.69 $\pm$ 2.8	0.3122
Gender			
Male	12	10	
Female	6	6	
BMI (kg/m <sup>2</sup> )	22.92 $\pm$ 0.7	22.44 $\pm$ 1.0	0.6934

expressed the AdipoR1 and AdipoR2 proteins. The expression levels of the AdipoR1 (Fig. 1B) and AdipoR2 (Fig. 1C) proteins were not significantly different between the control and the cancer patients.

**Gene expression analysis of *AdipoR1* and *AdipoR2*.** The expression levels of *AdipoR1* and *AdipoR2* mRNA were determined with a real-time RT-PCR assay (Fig. 2). All

samples expressed *AdipoR1* and *AdipoR2* mRNA. The levels of expression of *AdipoR1* (Fig. 2A) and *AdipoR2* (Fig. 2B) were not significantly different between the control and cancer specimens. In comparison with liver mRNA, the expression levels of normal colon epithelium *AdipoR1* and *AdipoR2* were 33.5 and 22.8%, respectively. The *AdipoR1* and *AdipoR2* expression levels in CRC were 19.9 and 14.4%, respectively (data not shown). In comparison with skeletal muscle mRNA, the expression levels of normal colon epithelium *AdipoR1* and *AdipoR2* were 13.1 and 13.5%, respectively. Expression levels of CRC *AdipoR1* and *AdipoR2* were 7.8 and 7.9%, respectively (data not shown). We also performed the full-length sequences of AdipoRs in cancer samples, though we could not find any mutation or deletion in these coding genes (data not shown). We investigated the relationship between plasma adiponectin concentration and the expression levels of the two AdipoRs, however we could not find any correlation between them (data not shown).

**Laser microdissection and real-time RT-PCR of *AdipoR1* and *AdipoR2*.** Colonic epithelial cells and cancer cells were collected from three patients with cancer. All cell samples expressed *AdipoR1* mRNA (Fig. 3A) and *AdipoR2* mRNA (Fig. 3B). The expression levels of *AdipoR1* and *AdipoR2*

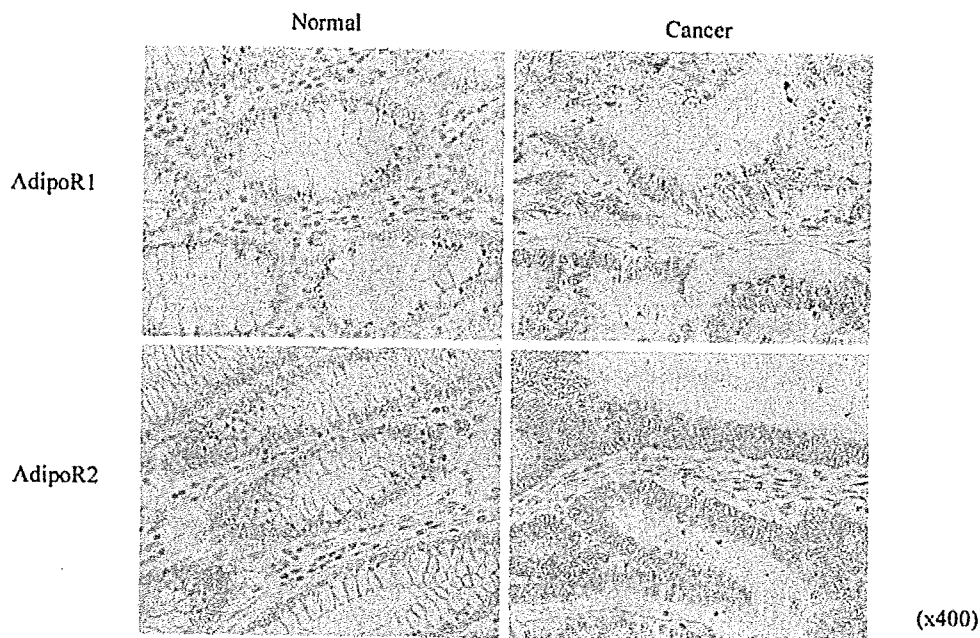


Figure 4. Immunohistochemical staining of AdipoR1 and AdipoR2 in normal and cancer tissue. AdipoR1 and AdipoR2 may be expressed in normal colonic epithelial cells and cancer cells. Concerning AdipoR1 and AdipoR2, strong staining of the cytoplasm can be observed in normal epithelial cells, primarily localized in the middle of the cells. Staining of a similar intensity is observed in cancer cells and normal cells.

mRNA were not significantly different between the normal cells and cancer cells.

**Immunohistochemical staining of AdipoR1 and AdipoR2.** We evaluated the localization of the expression of the AdipoRs using immunohistochemical staining. AdipoRs were expressed in normal colonic epithelial cells and cancer cells (Fig. 4). Strong staining of the cytoplasm was observed in normal epithelial cells for AdipoR1 and AdipoR2, primarily localized in the vicinity of the nuclei. Staining of a similar intensity was observed in cancer cells and normal cells. In the cancer cells, diffuse cytoplasmic staining patterns were observed.

## Discussion

In a prospective case-control study, Wei *et al* showed that men with lower plasma levels of adiponectin had a higher risk of CRC than those with higher plasma levels of adiponectin (12). In contrast, Lukanova *et al* reported finding no association between the plasma levels of adiponectin and the risk of CRC (13).

While some clinical studies regarding the plasma levels of adiponectin and CRC have been conducted on humans, no study has yet investigated the expression of the adiponectin receptors in normal colon epithelium and CRC tissues.

In the present human study, we clearly demonstrated the expression of adiponectin receptors, AdipoR1/AdipoR2, in normal colon epithelium and colon cancer cells. We confirmed our results at the genetic and protein expression levels and we further confirmed our results with laser microdissection. We could not find any mutation or deletion of the genes in the AdipoRs in this study. These results suggest the possibility that adiponectin may modulate the growth of normal colon

epithelial and CRC cells directly through AdipoR1 or AdipoR2.

In order to identify the cell types which express the adiponectin receptors, we performed immunohistochemical staining using antibodies for the two AdipoRs and we showed the expression of these receptors in normal colon epithelial cells and CRC cells. These results being further confirmed by the laser microdissection analysis.

In regard to the relative expression ratios of *AdipoR1* and *AdipoR2*, the gene expression analysis showed they were equally expressed. Although the expression levels of *AdipoR1* and *AdipoR2* in the colon were lower in comparison to liver and skeletal muscle mRNA, it was sufficient to induce some effects.

In our study, we could not find any significant difference in the expression levels of the two AdipoRs between normal colon epithelium and CRC tissues. Notably, we were able to demonstrate the expression of AdipoRs even in advanced carcinoma. These results raise the possibility that adiponectin plays an important role in the promotion of colon cancer.

We showed that the two AdipoRs were expressed in advanced CRC tissues. These results suggest the possibility that the AdipoRs might be a novel therapeutic target for the treatment of CRC. Further study of the roles of adiponectin and the AdipoRs in normal colon epithelium and CRC should therefore be conducted and the downstream mechanism of the AdipoRs need to be elucidated.

In conclusion, we clearly demonstrated that the two adiponectin receptors, AdipoR1 and AdipoR2, were expressed in normal colon epithelium and CRC tissues using real-time RT-PCR analysis, Western blotting, laser microdissection analysis and immunohistochemical staining. To the best of our knowledge, this is the first study that demonstrates the